LOCAL VARIATION AND REGIONAL TRANSPORT OF TROPOSPHERIC OZONE OVER CAPE TOWN

Master's dissertation

by

Claude-Michel Nzotungicimpaye

NZTCLA001

Presented towards the degree of Master of Science

in Environmental and Geographical Science

University of Cape Town

University of Cape Town

December 2013

Supervisor: Dr. Babatunde J. Abiodun

The copyright of this thesis vests in the author. No quotation from it or information derived from it is to be published without full acknowledgement of the source. The thesis is to be used for private study or non-commercial research purposes only.

Published by the University of Cape Town (UCT) in terms of the non-exclusive license granted to UCT by the author.

Abstract

The attractive image of Cape Town is threatened by periods of poor air quality occurring most often between April and September, during episodes of brown haze. When this haze occurs, it appears in the morning as a layer of concentrated pollution, likely to be associated with photochemical pollutants such as tropospheric ozone (O_3) and some of its precursors. Previous studies have identified local emission sources and meteorological conditions associated with both the air pollution and the brown haze in Cape Town. However, due to the transport of air pollutants, emissions from remote sources may also contribute to air pollution levels in Cape Town.

This dissertation investigates the local variation and the regional-scale transport of atmospheric pollution over Cape Town, with a focus on O_3 pollution. The study analyses O_3 observations from local air quality stations and uses two atmospheric chemistry-transport models to simulate the photochemical pollution over southern Africa.

The results show that the diurnal variation of O_3 in the Cape Town area is mainly driven by photochemical production while the seasonal variation is strongly associated with prevailing wind conditions. Surprisingly, the highest concentration of O_3 is observed at a remote background site (Cape Point) while the lowest concentration is observed at a sub-urban site (Goodwood) where there are chemical sinks of O_3 such as NO_x.

Atmospheric simulations show that extreme O_3 levels over Cape Town can be caused by air pollution transported from the industrial Highveld of South Africa, which is the principal source area of anthropogenic emissions in the country. Clusters of forward trajectories suggest four paths by which polluted air parcels from the industrial Highveld can be transported to Cape Town: a direct northeasterly path which is the most frequent route, a tropical deviation route, a deviation along the southern coastline of South Africa and an oceanic deviation path which is the least frequent route. Most of these trajectories (>70%) are simulated to occur between April and September, a period known to be characterized by poor ventilation conditions and the brown haze in Cape Town. This result suggests that the regional atmospheric transport between April and September contributes to increased air pollution levels over Cape Town.

Therefore, the study recommends the consideration of regional-scale emissions and atmospheric transport in monitoring the air quality of Cape Town, bearing in mind that the advection paths associated with critical levels of air pollution over Cape Town are the direct northeasterly path and the path along the southern coastline of the country.

Declaration

I hereby declare that this dissertation is my own work and that, to the best of my knowledge, it contains no material previously published or written by another person nor material which has been accepted for the award of any other degree or diploma of the university or other institute of higher education, except where due acknowledgement has been made in the text.

Claude-Michel Nzotungicimpaye

December 24, 2013

Dedication

To

Zoey Karezi Nzotungicimpaye

Acknowledgements

There are a lot of people that I would like to acknowledge for their support while I was conducting this study. The most important person is Dr. Babatunde J. Abiodun, my supervisor, who has been guiding me towards the achievement of this work. I acknowledge him for his enriching advice, critical review and trust in my abilities. I also thank him for introducing me to atmospheric models which I intend to keep on using in the future. I would also like to thank Prof. Douw G. Steyn who introduced me to the field of atmospheric science while I was just interested in statistical and mathematical modeling in a broad sense. I am grateful for his continued support throughout my graduate studies.

I also take this opportunity to acknowledge the institutions that provided financial support for my graduate studies at the University of Cape Town (UCT): the African Institute for Mathematical Sciences (AIMS), the UCT Postgraduate Centre and Funding Office (PGFO), and the UCT Science Faculty. My special acknowledgements go to A'eeda Rhodes, Olivia Barron, and Shahieda Samsodien who provided administrative assistance.

My gratitude also goes to the institutions from which I obtained real-time air quality and wind measurements that I analyzed in this work. Firstly, the City of Cape Town Air Quality Monitoring Section through Sally Benson and Fazlin Waggie; secondly, the scientific team in charge of ozone monitoring at the Global Atmosphere Watch station at Cape Point, namely Ernst-Günther Brunke and

Thumeka Mkololo; and thirdly, the South African Weather Service through Phumudzo Tharaga.

A substantial part of this work would not have been possible without an access to supercomputing systems. I thank the Climate System Analysis Group (CSAG) for providing me with access to its High Performance Computing facilities and technical support through its staff members, mostly Rodger Duffett and Phillip Mukwenha.

I benefited a lot from interacting with graduate students in my department but mostly with my officemates Eva L. Ujeneza and Samantha L. Jenner. I acknowledge the latter for substantial outputs from atmospheric models that I used in this study. Lawal A. Kamoru and Stefaan Conradie are acknowledged for commenting and proofreading this dissertation. I also thank Thomas Slingsby from the UCT GIS Lab for his support in creating one of the maps included in this document.

I cannot forget to thank my family members — namely Joachim, Marianne, Isaac, Iris, Augusta, Charles and Chanisse — for their encouragement during my studies. I also thank Larissa for her patience and emotional support. On the whole, I believe that all these people and opportunities were not just luck; hence I am very grateful to the Almighty.

List of Figures

List of Tables

Table of Contents

Chapter 1: Introduction

1.1 Tropospheric ozone

Atmospheric ozone (O_3) is a trace gas that exists in both the stratosphere and the troposphere. However, its effects differ in the two layers of the atmosphere. While stratospheric O_3 protects life on Earth against harmful ultraviolet radiations from the sun (The Royal Society, 2008), tropospheric O_3 contributes to climate forcing because it is a greenhouse gas (Unger et al., 2009; Stevenson et al., 2006). Apart from being a greenhouse gas, tropospheric O_3 is an air pollutant that has the potential to cause negative effects on natural vegetation (Paoletti, 2009; van Tienhoven, 2006), crop yields (Avnery et al. 2011), materials (Massey, 1999; Lee et al., 1996) and human respiratory, eye and cardiac health (WHO, 2006; Lippman, 1989; Ferris, 1978).

However, in contrast to many other air pollutants, tropospheric O_3 is not emitted into the atmosphere but is produced after a series of sunlight-driven chemical reactions that involve other air pollutants emitted from anthropogenic, biogenic and pyrogenic sources. These pollutants include nitrogen oxides (NO_x=NO+NO_2), volatile organic compounds (VOCs), carbon monoxide (CO) and methane (CH_4) (Atkinson, 2000; Collins et al., 2000; Crutzen and Zimmerman, 1991). Nevertheless, NO_x and VOCs are considered to be the principal precursors of O_3 in the lower troposphere (Sillman, 1999).

It is challenging to describe all the reactions between O_3 and its precursors, mainly because most of these reactions are nonlinear, but also because there is a huge diversity of VOC species. Nonetheless, by representing VOCs as RH (hydrocarbons in the form of R-H), a series of chemical reactions leading to formation of O_3 in the presence of VOCs and OH radicals can be described as initialized by the following reactions (Dickerson et al., 1997):

$$RH + OH \rightarrow H_2O + R \quad \text{(R1)}$$

$$R + O_2 \rightarrow RO_2 \quad \text{(R2)}$$

In the presence of NO_x and sunlight ($h\nu$), the RO_2 radicals generated in (R2) react with nitric oxide (NO) to generate O_3 as follows:

$$RO_2 + NO \rightarrow RO + NO_2 \quad \text{(R3)}$$

$$NO_2 + h\nu \rightarrow NO + O \quad \text{(R4)}$$

$$O + O_2 + M \rightarrow O_3 + M \quad \text{(R5)}$$

where M is an inert molecule required to carry away the energy released during the production process. Even though nitrogen oxides (NO_x) contribute to the formation of O_3, high levels of NO_x can induce the removal of O_3 as illustrated by the following sequence of reactions (Salby, 1996):

$$O_3 + NO \rightarrow NO_2 + O_2 \quad \text{(R6)}$$

$$NO_2 + O \rightarrow NO + O_2 \quad \text{(R7)}$$

with the following net effect

$$O_3 + O \rightarrow 2O_2 \quad \text{(R8)}$$

Such a removal of O_3 by NO_x is commonly known as "*the NO_x titration effect*" and it is recurrent in environments where traffic emissions are intense (The Royal Society, 2008). Furthermore, molecules of O_3 can also be destroyed by photolysis as indicated by the following reaction:

$$O_3 + h\nu \rightarrow O_2 + O(^1D) \quad \text{(R9)}$$

where $O(^1D)$ represents very excited atoms of oxygen that are able to react with many compounds in the troposphere (Crutzen et al., 1999; Crutzen, 1974). In the presence of water vapor, the $O(^1D)$ atom can contribute to the formation of the hydroxyl radical (OH) as indicated by the reaction:

$$H_2O + O(^1D) \rightarrow 2OH \quad \text{(R10)}$$

The removal of O_3 through reactions (R9) and (R10) is efficient in environments where O_3 precursors are scarce (The Royal Society, 2008). Otherwise, in the presence of enough VOCs and NO_x, the OH radicals generated through the reaction (R10) may contribute to the regeneration of O_3 through the process (R1)-(R5).

Ozone is a common pollutant in urban and industrial environments because most of the O_3 precursors (namely NO_x, CO and VOCs) are emitted by traffic and industries (The Royal Society, 2008; Collins et al., 2000). In addition, O_3 is a major component of the urban smog (Sillman, 2003) that pollutes the atmosphere of many cities across the globe. Therefore, it is relevant to investigate O_3 pollution in urban environments, especially in cities that experience poor air quality such as Cape Town.

1.2 Poor air quality in Cape Town

Cape Town is a coastal city located at the southwestern tip of Africa. The metropolitan area of Cape Town covers approximately 2,500 km^2 and is home to nearly 4 million people (City of Cape Town, 2012). Anthropogenic activities in the Cape Town area contribute to the emission of trace gases, aerosols and particulate matters that are associated with air pollution episodes observed in the city (City of Cape Town, 2013; Scorgie and Watson, 2004). The major contributors to these emissions are from traffic activities, although domestic and industrial emissions contribute significantly over localized zones (Piketh et al., 2004; Walton, 2005; Chiloane, 2005; Wicking-Braid et al., 1997). However, some industrial areas that were initially located on the peripheries of the city are now surrounded by residential areas following the city expansion (Sowden et al., 2008), making it hard to distinguish the sources of emissions but also enhancing the human exposure to polluted air. The impacts of human exposure to air pollution in Cape Town include increasing mortality due to respiratory, cardiovascular and cerebrovascular diseases (Wichmann and Voyi, 2012).

Although the Cape Town area is not as large as most of the world's megacities and, despite that it is located near a clean marine environment, it experiences an unusual smog pollution locally known as "*the brown haze*". This haze is recurrent between April and September; and when it occurs, a polluted layer extends over most of the metropolitan area in such a way that the atmosphere over Cape Town becomes heavily polluted; resulting in visibility degradation and extreme pollution levels (Piketh et al., 2004).

In order to reduce the health effects of poor air quality on its inhabitants, especially during brown haze episodes, the City of Cape Town operates a dozen air quality monitoring stations, spread across the metropolitan area. Additionally, the municipality controls local vehicle emissions and contributes to the improvement of air quality in informal settlements (City of Cape Town, 2005). Certainly, local atmospheric emissions contribute significantly to the formation of the brown haze. However, air pollutants from sources outside the Cape Town area might also be contributing to the levels of air pollution in the city. This study investigates the regional-scale transport of air pollutants over Cape Town, with a focus on O_3 pollution.

1.3 Study aim and objectives

The aim of this study is to investigate the local variation and the regional-scale transport of O_3 pollution over Cape Town. The objectives of the study are as follows:

- To describe the local variation of ground-level O_3 in the Cape Town area, especially with respect to local emissions and wind conditions.
- To simulate the atmospheric pollution over southern Africa using two atmospheric chemistry-transport models (RegCM-Chem and WRF-Chem).
- To evaluate the ability of the two atmospheric models in simulating the photochemical pollution over Cape Town.
- To study the regional transport of O_3 pollution and its implications on air quality in Cape Town.

- To identify the possible advection paths by which polluted air parcels from a particular remote source are transported to Cape Town.

1.4 Dissertation outline

This dissertation is divided into seven chapters. Chapter 2 provides a review of the literature on the evidence and the impacts of large-scale transport of O_3 pollution as well as the distribution of tropospheric O_3 over southern Africa. Chapter 3 presents the observed data used to study the variation of ground-level O_3 in the Cape Town area. In addition, this chapter provides a description of the atmospheric models and their set-up, as well as the lagrangian trajectory model used to simulate the transport of air parcels from a remote source to Cape Town. The study results are presented in Chapters 4, 5 and 6. Chapter 4 discusses the local variation of ground-level O_3 in the Cape Town area. A validation of the two atmospheric models against observed data over Cape Town is presented in Chapter 5. Chapter 6 discusses the results on the regional-scale transport of O_3 pollution over South Africa and its impacts on the air quality over Cape Town. A conclusion and suggestions for further studies are presented in Chapter 7.

Chapter 2: Literature review

2.1 Long-range transport of O_3 pollution: evidence and impacts

Although O_3 precursors are mostly emitted in urban and industrial areas, certain rural areas experience high concentration of O_3 caused by long-range transport of O_3 and its precursors. For example, the O_3 episodes frequently observed during summer in northern Portugal (Monteiro et al., 2012) and Spain (Saavedra et al., 2012) have been associated with O_3 pollution transported from urban and industrial areas of the Iberian Peninsula (Borrego et al., 2013). Due to the long-range atmospheric transport, O_3 pollution is also advected across national borders, making O_3 an important transboundary pollutant (The Royal Society, 2008). For instance, Brankov et al. (2003) studied the transport of O_3 pollution between New York City and Toronto and showed that air parcels from each of the two cities can cross national borders, contributing to O_3 pollution in the neighboring country. Furthermore, Yoshitomi et al. (2011) showed that, during springtime, emissions from China contribute to an increase of 2-6 parts per billion (ppb) O_3 levels in Japan. In southern Africa, the transport of biomass burning products from tropical Africa contributes to the seasonal maxima O_3 concentrations observed over most of Botswana, Namibia, Zimbabwe and parts of northern South Africa (Thompson et al., 1996a; 1996b).

The long-range transport of O_3 pollution can surpass the continental limits to extend over hemispheric scales, making O_3 a pollutant of global concern (The Royal Society, 2008; Stohl, 2002). Although the inter-continental transport of O_3 and its precursors may take up to 2 weeks (Liu and Mauzerall, 2005), it

contributes to increased concentration over the receptor continent. For example, in the northern hemisphere, Duncan et al. (2008) showed that long-range transport of pollution from Europe contributes to increased O_3 levels over northern Africa and the Middle East, causing extreme O_3 levels on more than 50 days per year. In addition, Fiore et al. (2002) found that anthropogenic emissions in Europe and Asia contribute to increased surface O_3 concentration in the United States by 4–7 ppb in summer. Furthermore, springtime O_3 maxima levels in Europe have been associated with anthropogenic emissions from Asia and North America (Derwent et al., 2008; 2004). Li et al. (2002) found that the influence of emissions from North America on air quality in Europe is driven by the long-range transport of O_3 itself, rather than that of its precursors and suggested that 20% of the extreme O_3 pollution events in Europe in the summer of 1997 would not have occurred in the absence of anthropogenic emissions from North America.

Compared to the northern hemisphere, fewer studies have investigated the intercontinental transport of O_3 and its precursors in the southern hemisphere. Using trajectory modeling, Thompson et al. (1996a) suggested that air parcels rich in O_3 off the northeastern coast of Brazil reach southwestern Africa during the season of biomass burning, and contribute to the seasonal O_3 maxima levels over the tropical Atlantic Ocean. Furthermore, Wenig et al. (2003) detected a plume rich in NO_2 stretching from the eastern South Africa to Australia, from GOME[1] satellite imageries; pointing out the potential implication of South African

[1] GOME: Global Ozone Monitoring Experiment

emissions on photochemistry over the South Indian Ocean. This observation by Wenig et al. (2003) confirmed the results in Sturman et al. (1997) which showed that air parcels from eastern South Africa can be transported as far as Oceania.

The results from these studies show that, even though the long-range transport of O_3 and its precursors may be occasional and its contribution to increased local ambient concentration may be of the order of a few units only, it might still contribute to the exacerbation of air quality in locations downwind. The findings from these studies highlight the necessity of monitoring O_3 pollution at the regional scale.

2.2 The distribution of tropospheric O_3 over southern Africa

Research started to give attention to the distribution of tropospheric O_3 over southern Africa when Fishman et al. (1986; 1990; 1991) identified, using TOMS[2] satellite observations, seasonal maxima of total column O_3 over the tropical southeast Atlantic and southern Africa each year between August and October. These observations gave rise to international research initiatives with the aim of putting together a regional picture of the distribution of tropospheric O_3 (Thompson et al., 1996a). Because fire emissions prevail over most of tropical Africa and South America during these months, it was assumed that the regional O_3 maxima levels were linked to biomass burning products released from these land areas (Fishman and Larsen, 1987). Therefore, one of the objectives of these research initiatives was to investigate the transport of pollution from biomass burning source areas to the locations where O_3 maxima levels were observed

[2] TOMS: Total Ozone Monitoring Spectrometer

(Thompson et al., 1996a). These research initiatives used various atmospheric sampling tools that include ground-measurements, ozonesondes and aircraft campaigns. During September and October 1992, the first aircraft campaigns to focus on the aspects of O_3 and associated dynamics over southern Africa took place as part of SAFARI-92[3] (Andrea et al., 1994). Several studies (such as Thompson et al., 1996a; Thompson et al., 1996b; Garstang et al., 1996; Diab et al., 1996; Cosijn and Tyson, 1996; Swap et al., 1996, etc.) that resulted from SAFARI-92 were published in a special issue of the *Journal of Geophysical Research* (vol. 101, no. D19, 1996). Thompson et al. (1996a) combined trajectory and photochemical modeling to show a connection between the seasonal O_3 maxima levels observed over southern Africa and biomass burning products from Angola, Zambia and Mozambique, that are recirculated over the subcontinent under the influence of a semi-permanent continental anticyclone. A key result of SAFARI-92 was that southern Africa is a network of biogeophysical systems linked by regional atmospheric circulation, and that biomass burning products were the principal but not the only significant source of O_3 precursors during the spring O_3 maxima over the subcontinent (Thompson et al., 1996a). Later on, however, Swap et al. (2003) suggested that the contribution from biogenic and anthropogenic emissions in southern Africa to the regional spring O_3 maxima levels might also be substantial.

Besides the biomass burning emissions that are seasonal, anthropogenic emissions from urban and industrial areas in southern Africa are permanent and

[3] SAFARI: Southern Africa Fire Atmospheric Research Initiative

contribute to the less homogeneous distribution of O_3 over the subcontinent. For example, over South Africa, Combrink et al. (1995) compared the variation of O_3 concentration from two sites near industries (Elandsfontein and Verkykkop) in the north-eastern Highveld to O_3 concentration from Cape Point, a coastal and remote background site away from intense human activity, at the south-western tip of the country. Their results showed that both the diurnal and seasonal variations of O_3 concentration were different in the two areas. While the O_3 concentration at Cape Point features a weak diurnal cycle, the diurnal cycle of O_3 concentration near the industrial area increases following peak emission hours. In addition, the seasonal cycle of O_3 concentration at Cape Point peaks (~28 ppb) in winter, whereas the seasonal O_3 maxima levels (>40 ppb) in the industrial area occur in spring (usually in September), possibly owing to both the industrial and the seasonal fire emissions.

A larger set of station data from across southern Africa were analyzed by Zunckel et al. (2004) under the CAPIA[4] project. The aim of the project was to assess the potential risk of damage that O_3 can cause to maize crops over southern Africa. Consequently, their study only considered data from monitoring stations outside of urban and industrial areas. Ozone data from ten sites (eight in South Africa, including six from the north-eastern Highveld of the country; one site in Etosha, Namibia; and a site in Maun, Botswana) were analyzed in their study. With the exception of O_3 levels from Cape Point that is primarily influenced by air masses of marine origin (Zunckel et al., 2004; Brunke et al., 2004), surface

[4] CAPIA: Cross Border Air Pollution Impact Assessment

O_3 concentrations at the other nine sites featured strong seasonal variations, with maxima occurring between August and October, due to biomass burning products during this season (Zunckel et al., 2004). Furthermore, the highest O_3 concentrations were reported at Maun (northern Botswana) and at the sites in the north-eastern Highveld of South Africa. In both areas, springtime O_3 maxima varying between 40-60 ppb were recorded, exceeding the threshold O_3 concentration of 40 ppb, which was considered to represent a risk for maize crops (Zunckel et al., 2004).

However, because these monitoring stations were not necessarily located in areas where maize is grown, the CAPIA project adopted the use of photochemical modeling to complement the work of Zunckel et al. (2004) (Zunckel et al., 2006; van Tienhoven et al., 2006). By coupling two Eulerian models (MM5 for meteorology and CAMx for photochemistry), Zunckel et al. (2006) simulated the distribution of O_3 over southern Africa for 5 days each month during the maize growing season of October 2000 to April 2001. Their model results showed that parts of Namibia, Botswana, Zambia, Zimbabwe, Mozambique and South Africa experience maxima O_3 levels above the fixed threshold. In South Africa, the highest O_3 concentration was simulated over the north-eastern Highveld, which covers the most urbanised and industrialised areas of the country (Collett et al., 2000). Several studies (such as Zunckel et al., 2000; Collett et al., 2000) showed that this region is the principal source area of anthropogenic emissions (including O_3 precursors) of the country and a major one worldwide (Munnik et al., 2010; Wenig et al., 2003), from where air parcels

are transported to various locations downwind, on the subcontinent and over the adjacent oceans (Freiman and Piketh, 2002).

2.3 Transport of air parcels out of the industrial Highveld

Previous studies (such as Cosijn and Tyson, 1996; Garstang et al., 1996) have shown that the vertical transport of air parcels over the Highveld region of South Africa is prevented by three stable atmospheric layers. These layers occur primarily under subsidence imposed by the descending branches of the Ferrell and Hadley cells near the southern mid-latitudes (Garstang et al., 1996). The top layers around 300 hPa (~7 km) and 500 hPa (~5 km) are semi-permanent throughout the year, while the lowest layer at 700 hPa (~3 km) is occasionally disrupted, allowing air parcels to move upward and get trapped between the 700 and 500 hPa layers. In general, the mixing height is increased in summer by surface heating (Tyson et al., 1997) and the atmospheric conditions over the Highveld tend to be more stable in late autumn, winter and early spring (Preston-Whyte et al., 1977). When these atmospheric layers inhibit vertical transport, air pollution from the industrial Highveld is constrained to the horizontal transport within the lowest layers of the troposphere.

Freiman and Piketh (2002) used trajectory modeling to investigate the transport of air parcels out of the industrial Highveld. By running trajectories for 4 months (February, April, July and October) over 8 years, from a five-point array centered over the industrial Highveld, at 800 and 700 hPa, these authors identified two major modes for zonal transport of air parcels out of the Highveld.

The first mode consists of recirculated transport, by which polluted air recirculates in an anticyclonic pattern back towards the point of origin over the subcontinent. This recirculation can occur on both regional and subcontinental scales. Depending on the scale of the recirculation, the transport time ranges from two to nine days. On average, a third (33%) of all transport was estimated to be recirculated over the interior subcontinent (Freiman and Piketh, 2002). Piketh et al. (2002) provided the evidence of the passage of recirculated pollution from the industrial Highveld at Ben MacDhui, a site located in southern Lesotho.

The second mode is direct transport in which polluted air from the industrial Highveld is transported directly to various locations downwind, representing 67% of all transport (Freiman and Piketh, 2002). Most of the air transported out of the industrial Highveld (45% of all transport) exits the subcontinent towards the southwest and south Indian Ocean. Occasionally, air parcels exiting the subcontinent in this way reach places as distant as Oceania (Wenig et al., 2003; Sturman et al., 1997). Direct transport out of the Highveld also accounts for 14% cases towards the Atlantic Ocean and 8% cases towards the equatorial Africa (Frieman and Piketh, 2002). Under stable conditions, polluted air parcels from the Highveld can reach equatorial countries, as distant as Kenya (Tyson and Gatebe, 2001). Therefore, it is evident that aerosols and trace gases from the industrial Highveld can be transported over hundreds to thousands of kilometers across the subcontinent and the adjacent marine areas. It is also possible that these polluted air parcels contribute to worsen the air quality in remote locations including cities such as Cape Town.

2.4 Characterization of air pollution in Cape Town

2.4.1 Meteorological aspects

The levels of air pollutants in Cape Town depend on prevailing meteorological conditions. During the haze months (April to September), synoptic conditions in the upper troposphere are dominated by anticyclonic circulations associated with a continental high-pressure system over southern Africa (Tyson et al., 1996). This circulation pattern induces subsidence of air over most of the subcontinent, resulting in stable conditions in the lower troposphere. Jury et al. (1990) suggested that such stable conditions and the steep topography in Cape Town enhance the accumulation of air pollutants and the formation of the brown haze. In addition, Jury et al. (1990) found that the haze pollution is associated with berg winds that reach Cape Town by the north-eastern route. These winds are slow and can blow for hours to days (Preston-Whyte and Tyson, 1988), promoting the accumulation of air pollutants over Cape Town. Piketh et al. (2004) identified similar northeasterly winds during the brown haze season.

Unlike over the interior South Africa (see in Section 2.3), coastal regions (including Cape Town) experience near-surface stable conditions, caused by subsidence of air (Cosijn and Tyson, 1996). Using radiosonde soundings from the Cape Town International Airport, Piketh et al. (2004) identified stable layers that occur between 900 hPa (<1 km) and 750 hPa (2.5 km), in agreement with Cosijn and Tyson (1996) who showed that coastal areas of South Africa experience absolute stable layers around 850 hPa (~1 km). These layers were found to be important factors that contribute to the accumulation of air pollutants

during the haze season in Cape Town (Piketh et al., 2004). However, Keen (1979) observed that the haze pollution in Cape Town is more commonly associated with nocturnal temperature inversions than with the elevated subsidence inversions. Wicking-Baird et al. (1997) agrees with both Keen (1979) and Jury et al. (1990) by showing that brown haze episodes in Cape Town are often associated with both nocturnal temperature inversions and berg winds over Cape Town.

Nonetheless, there also exist meteorological conditions that contribute to the reduction of air pollution in Cape Town. In winter, westerly disturbances over the west coast of South Africa have a cleansing effect on air over Cape Town (Wicking-Baird et al., 1997; Preston-Whyte and Tyson, 1988). During summer, strong southeasterly winds (locally known as "*The Cape Doctor*") dilute the atmosphere, resulting in low levels of pollution over most of the Cape Town area. In autumn, cool air advected by the cold Benguela Current tends to dilute the atmosphere over the city (Jury and Spencer-Smith, 1988). Other circulation patterns such as sea breezes, also contribute to the atmospheric dilution over Cape Town (Keen, 1979).

2.4.2 Sources of atmospheric emissions

Apart from the influence of meteorological conditions, poor air quality conditions in Cape Town are associated with atmospheric emissions. Various methods have been used to identify local sources of these emissions. Using ground-based measurements collected between 1995 and 1996, Wicking-Braid et al. (1997)

attributed 65% of the visible degradation caused by the brown haze to vehicle emissions and 22% of it to local industrial emissions. The use of wood, most common in informal settlements and townships (City of Cape Town, 2002), contributes 11% to the visible degradation, while the contribution from natural sources such as sea salt and wind-blown dust was estimated at only 2% (Wicking-Braid et al., 1997). In order to study the composition of the brown haze, Piketh et al. (2004) used aircraft samplings and identified high levels of primary pollutants (e.g. NO and SO_2) over industrial areas and high levels of O_3 near Strand, a location on the south-east coast of the Cape Town area. With the same aircraft measurements, Chiloane (2005) found the highest levels of VOCs over the north-east of the Central Business District (CBD), Wallacedene, Grassy Park and the township of Mitchell's Plain. Moreover, substantial anthropogenic emissions in the township of Khayelitsha contribute to the most frequent and severe episodes of particulate matters (i.e. PM_{10}) in the Cape Town area (City of Cape Town, 2013; City of Cape Town, 2012; Tessema, 2011; City of Cape Town, 2005). Furthermore, Walton (2005) used a Eulerian model to show that major sources contributing to the visibility degradation during brown haze episodes are the CBD, the Caltex Oil Refinery near Tableview and the townships of Mitchell's Plain and Khayelitsha.

However, few studies have investigated the contribution of emissions from remote sources to the poor air quality in Cape Town. Recent studies by Abiodun et al. (2013) and by Jenner and Abiodun (2013) suggested a link between extreme pollution levels in Cape Town and air pollution transported from the

Mpumalanga Highveld. However, Jenner and Abiodun (2013) only focused on the transport of sulfur compounds, while Abiodun et al. (2013) only studied the transport of nitric compounds without considering their influence on the local O_3 pollution. In addition, none of these studies identified the paths by which polluted air parcels from the industrial Highveld are advected to Cape Town. This study investigates these aspects of regional air pollution.

Chapter 3: Methodology

3.1 Observed data

In Chapter 1, it was mentioned that the City of Cape Town operates a dozen air quality stations in order to monitor air pollutants that have negative impacts on human health and contribute to brown haze. However, few of those stations monitor O_3 on a continuous basis. This study analyses data of ambient O_3 concentration obtained from two stations (Goodwood and Molteno) regulated by the municipality, and additional data from the GAW (Global Atmosphere Watch) station at Cape Point regulated by the SAWS (South African Weather Service). The geographical location of each of these three stations is shown in Figure 1.

The records of O_3 concentration at the three sites were obtained in different formats. While the O_3 readings from Molteno (33°93'S and 18°41'E) and Goodwood (33°54'S and 18°33'E) are recorded every hour, those from Cape Point (34°21'S and 18°29'E) are recorded every half-hour. In addition, the O_3 concentration at Molteno and Goodwood are recorded in microgram per cubic meter ($\mu g/m^3$) while the O_3 concentration at Cape Point is recorded in ppb. A conversion of the O_3 readings from Cape Point, from ppb to $\mu g/m^3$, then from half-hourly to hourly, is done to allow comparison between the O_3 levels at the three sites. Unfortunately none of the three stations monitor VOC species[5], while measurements of O_3 precursors (i.e. NO_x and CO) were only available from the Goodwood station. Therefore, NO_x and CO data from Goodwood are also used

[5] Having started in the mid 2000s, the monitoring of VOC species in the Cape Town area is currently conducted at one station (Foreshore) (Personal communication with Fazlin Waggie from the Air Quality Monitoring Section, City of Cape Town).

in this study, to investigate the role of emissions on the local variation of O_3 concentration.

Figure 1 Location of air quality monitoring stations within the Greater Cape Town area. Red squares on the map show sites from which O_3 and wind data were obtained for this study. Different colors are used to show the different suburbs of the Greater Cape Town area. Source: www.capetown.gov.za/airqual (with some modifications).

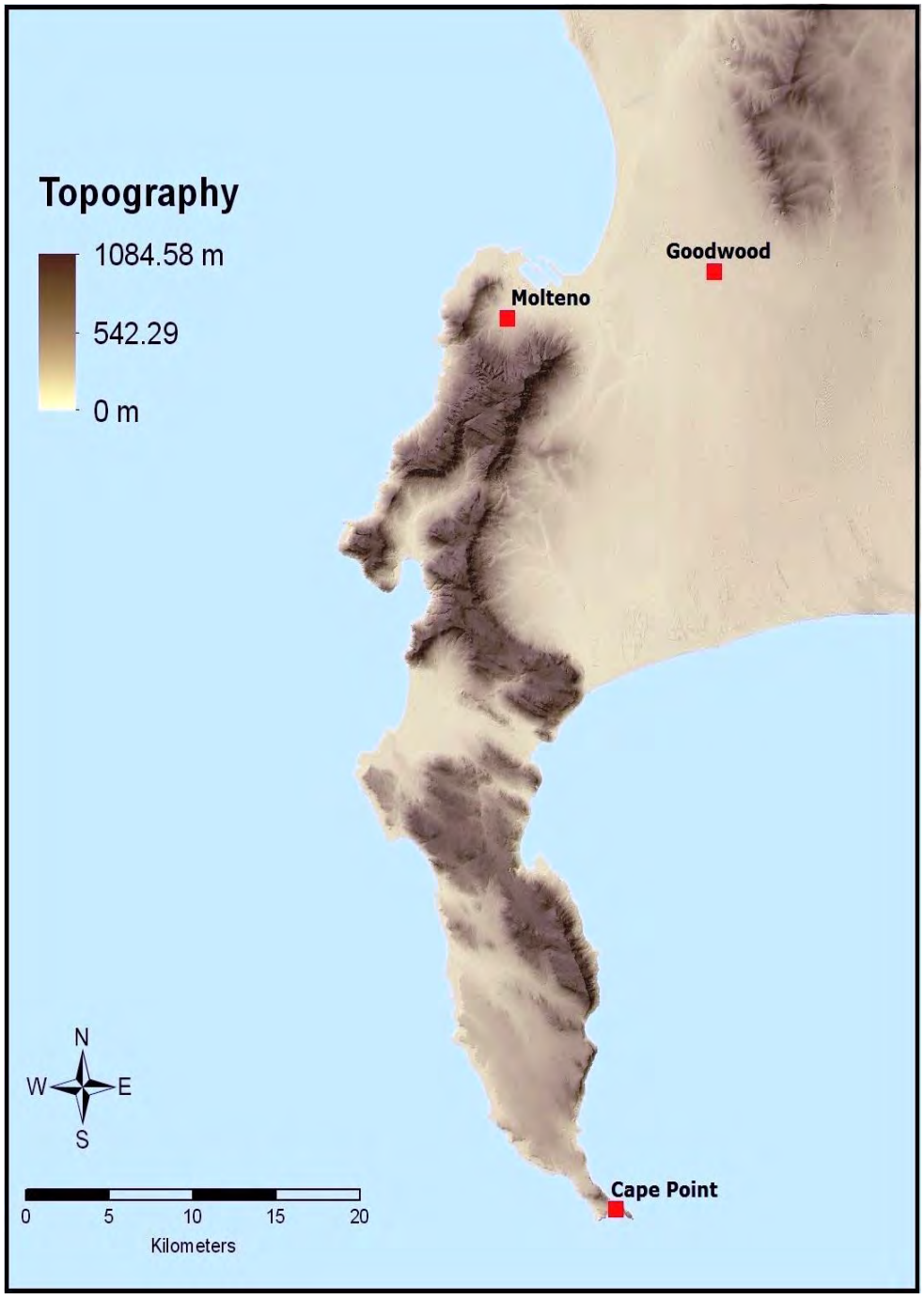

Figure 2 Topography near the air quality stations at Molteno, Goodwood and Cape Point. The map shows the topography of the Cape Peninsula as well as the location of the three sites from where air quality and wind data were obtained for this study. The approximated elevations at each site are the following: Molteno (98m), Goodwood (27m) and Cape Point (8m). The map was created with help from the University of Cape Town GIS Lab.

The distances between the three sites are as follows: Molteno – Goodwood (~16 km), Molteno – Cape Point (~65 km) and Goodwood – Cape Point (~77 km). The Goodwood station is located in a semi-residential and semi-industrial suburb traversed by busy roads such as the R102, the M7 highway and the N1 national road. Furthermore, there are informal settlements and small-scale industries to the south of Goodwood. Therefore, levels of air pollutants recorded at that station likely account for a mix of traffic, domestic and industrial emissions. The Molteno station is located in a residential area in the vicinity of the city centre. Thus, ambient air concentrations recorded at that station might be dominated by pollution from traffic emissions. The station at Cape Point is located at the southern of the Cape Peninsula, away from substantial human activity. Even though the site attracts local and international tourists, anthropogenic emission rates at the site are likely to be much lower than those at Molteno and Goodwood. In addition, the Cape Point station is the oldest O_3 monitoring site within the region, and several studies have been conducted to assess the variation of O_3 in such a clean environment (Oltmans, 1981; Scheel et al., 1990; Oltmans and Levy II, 1994).

In order to study the influence of wind conditions on O_3 pollution in the Cape Town area, hourly measurements of wind speed and wind direction were obtained from each of the three stations, but from different institutions. While wind data from Goodwood were obtained from the Air Quality Monitoring Section of the City of Cape Town, those from Molteno and Cape Point were obtained from SAWS. The topography near each of the three sites (Figure 2) can help

understanding the local air pollution dynamics. Goodwood is located in a flat environment that allows the flow of wind off the ocean and subsequent dispersion of air pollutants. In contrast, the station at Molteno is partially enclosed by mountains that might limit the effective dispersion of air pollutants. Consequently, air pollutants (locally emitted or produced and those transported) are likely to accumulate near this site, contributing to increasing the levels of air pollution. The station at Cape Point (on the southern edge of the Cape Peninsula) experiences winds of marine origin, which are likely to contribute to the dilution of the atmosphere. Air quality and wind readings for the period 2001-2004 from the three stations are used to describe the local variation of ground-level O_3 in the Cape Town area.

3.2 Simulation of the photochemical pollution over southern Africa

As in Cape Town, direct measurements of O_3 elsewhere in southern Africa are scarce, limited to a few active and passive stations (Zunckel et al., 2006). To overcome this scarcity of O_3 data in the region, we simulated the photochemical pollution over southern Africa using two atmospheric chemistry-transport models: RegCM-Chem (hereafter RegCM) and WRF-Chem (hereafter WRF). Using more than one model presents two major advantages: (a) an inter-model comparison becomes possible; (b) the robustness of the study results increases. The following sub-sections provide a description of the two atmospheric models, their parameterization and initialization in order to simulate the atmospheric pollution over southern Africa.

3.2.1 RegCM description, set-up and chemistry initialization

One model that this study uses to simulate the regional photochemical pollution is the International Centre for Theoretical Physics (ICTP) Regional Climate Model (RegCM), version 4. The RegCM is a hydrostatic and terrain-following coordinate model (Giorgi and Anyah, 2012; Pal et al., 2007) whose climate component has been successfully tested over South Africa (Sylla et al., 2009).

The climate module of RegCM has different parameterization schemes to represent atmospheric processes. For this study, the model uses the CCM3 scheme (Kiehl et al., 1996) for radiation calculations, the mass-flux cumulus scheme of Grell et al. (2005) with Fritsch and Chappell (1980) closure for convection, and the Holtslag and Boville (1993) parameterization for the boundary layer. Land-atmosphere interactions are parameterized according to the Biosphere-Atmosphere Transfer Scheme (BATS) (Dickinson et al., 1993) which is based on Monin-Obukhov similarity relations (Monin and Obukhov, 1954).

For the chemical processes, the model uses the Carbon Bond Mechanism, version Z (CBM-Z) (Zaveri and Peters, 1999) for gas-phase mechanisms and the Tropospheric Ultraviolet-Visible model (TUV) scheme (Madronich and Flocke, 1999) for photolysis. Dry deposition follows the Community Land Model 4 (CLM4) developed by Wesley (1989). A detailed description of the incorporation of gas-phase chemistry within RegCM is described in Shalaby et al. (2012).

Due to the lack of a gridded emission inventory for southern Africa, the RCP[6] global emission data were used to initialize the photochemistry within RegCM. While these emissions data are publicly available[7], they were obtained with the RegCM package. These emissions are available at a horizontal grid-resolution of 1° x 1°, and they account for the various O_3 precursors (Figure 3).

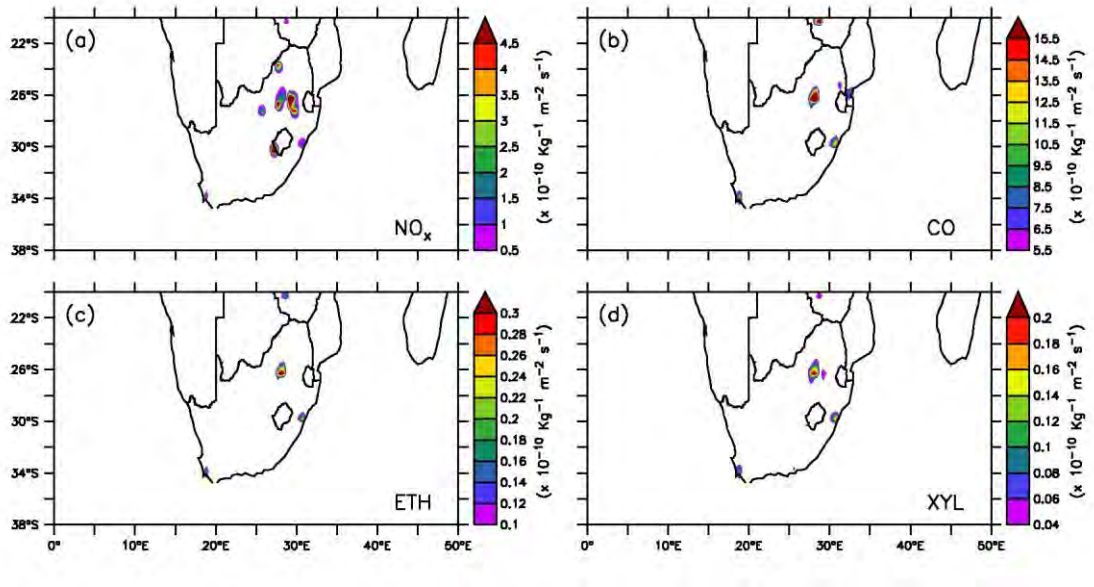

Figure 3 Emission rates of O_3 precursors over South Africa as used to initialize RegCM. Only some of the precursors are shown in the figure: (a) NO_x, (b) CO, (c) ethylene (VOC) and (d) xylenes (VOCs). These emission rates are as found in the RCP database.

Although the RCP emission data may not be accurate over southern Africa, they were used to meet the goal of the study which is to identify patterns in the regional transport of O_3 pollution to Cape Town. Furthermore, these emission inputs have monthly variation but no diurnal variation. Therefore, it is assumed

[6] RCP: Representation Concentration Pathways

[7] The RCP database is available online from the International Institute for Applied Systems Analysis (IIASA) based in Austria. More information about the emission database can be found at http://tntcat.iiasa.ac.at:8787/RcpDb/dsd?Action=htmlpage&page=about (2012)

that daily variations in simulated concentration of air pollutants are mainly driven by the variation in meteorological conditions.

3.2.2 WRF description, set-up and chemistry initialization

The other model used in this study is the non-hydrostatic Weather Research and Forecasting (WRF) model (Skamarock et al., 2005). As with RegCM, WRF is a terrain-following model and its climate component has been successfully tested over southern Africa (Crétat et al., 2011). In this study we used the WRF version 3.2, coupled with chemistry (WRF-Chem) to simulate the photochemical pollution over southern Africa. A full description of WRF-Chem is provided in Grell et al. (2005).

The model employed the RRTM (Rapid Radiation Transfer Model) for longwave radiation (Mlawer et al., 1997), the Dudhia (1989) shortwave radiation scheme, the Grell 3D ensemble cumulus scheme (Grell and Devenyi, 2002), and the Yonsei University scheme (YSU) for the planetary boundary layer (Hong et al., 2006). Similar parameterizations to those selected in setting up RegCM were used where possible for the photochemical processes in WRF. For instance, the model used the CBM-Z for gas-phase mechanism (Zaveri and Peters, 1999) and the Madronich scheme (Madronich, 1987) for photolysis. Dry deposition is resolved using the ‘‘flux-resistance’’ method (Wesley, 1989).

Again due to the lack of a gridded emission inventory for southern Africa, atmospheric emissions available at the global scale were used to initialize the

photochemistry in WRF; but this time the emission data were from EDGAR[8] version 4.2, available at a 1.5° x 1.5° resolution. This emission dataset was obtained separately from WRF and a pre-processing was required to make it readable by the model. Hence, the EDGAR emissions were firstly prepared using an open pre-processor described in Freitas et al. (2011). As for the RCP emissions, the EDGAR emission dataset includes various O_3 precursors (Figure 4).

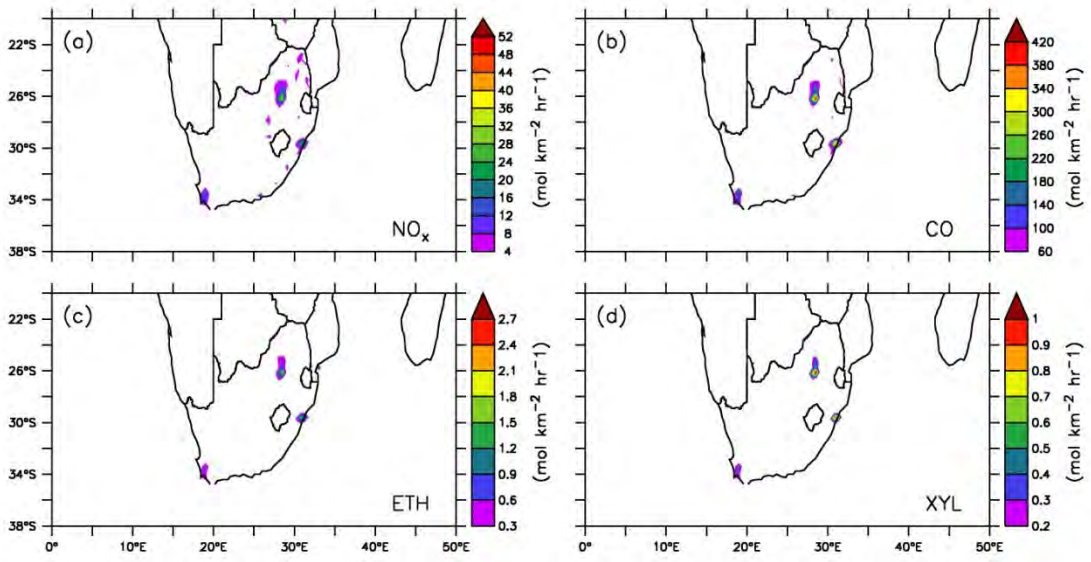

Figure 4 Emission rates of O_3 precursors over South Africa as used to initialize WRF. Only some of the precursors are shown in the figure: (a) NO_x, (b) CO, (c) ethylene (VOC) and (d) xylenes (VOCs). These emissions are as found in the EDGAR4.2 database.

[8] EDGAR: Emission Database for Global Atmospheric Research. This dataset is from the European Commission Joint Research Centre (JRC) in partnership with the Netherlands Environmental Assessment Agency (PBL). More information about the emission database can be found at http://edgar.jrc.ec.europa.eu (2011)

The reader should note that in both RCP and EDGAR datasets atmospheric emissions over Cape Town are substantial (Figures 3 and 4), suggesting that the Cape Town area is a potential source of O_3. Again as for the RCP emissions, the EDGAR emissions might not be accurate over southern Africa, but still they were used because the aim of the simulation is to allow an investigation of the regional-scale transport of O_3 pollution, and not the prediction of O_3 concentration in the region.

3.2.3 Meteorological initialization, domain and period of simulation for both models

For this study, it was crucial that both RegCM and WRF use reliable initial conditions for the atmospheric dynamics in order to expect good results from the simulation of the regional transport of air pollutants. Meteorological input (initial and boundary conditions) provided by the 6 hourly ERA-Interim 1.5° x 1.5° gridded reanalysis data from the ECMWF (European Centre for Medium-Range Weather Forecasting) were used for both models. This data has been assessed to be appropriate for studying the atmospheric transport (Piketh et al., 2002; D'Aberton, 1996; Thompson et al., 1996a) and the climatology (Sylla et al., 2009) over southern Africa.

The simulation domain was centered at 24°E and 33°S for both models. However, the domain size was slightly different for the two models. For RegCM, the simulation domain spanned the region between 16.62°W and 54.41°E (with 189 grid points), and between 10.50°S and 40.45°S (with 97 grid points). For WRF, the domain spanned the region between 16.69°W and 56.10°E (with 188

grid points) and between 12.82°S and 37.54°S (with 96 grid points). Nonetheless, both domains were subdivided into grids of 35 km resolution in the horizontal, following the Lambert conformal projection (Figure 5). The two models also had different stratification in the vertical. While RegCM uses 18 sigma layers, WRF uses 33 sigma layers. In both cases, the highest resolution is within the lowest layers (near the surface). In this study, the simulations for the lowest model grid level were assumed to represent the ground-level O_3 and near-surface wind conditions.

The simulation experiment is done for the period October 2000-December 2004, with both models. The experiment is limited to this period because of the limited computing resources available for this study. The simulation for the first 3 months (October-December 2000) is considered as model spin-up, and hence is discarded for the analysis. Therefore, only the analysis of the 48-month simulation from January 1st, 2001 to December 31st, 2004 is presented in this study.

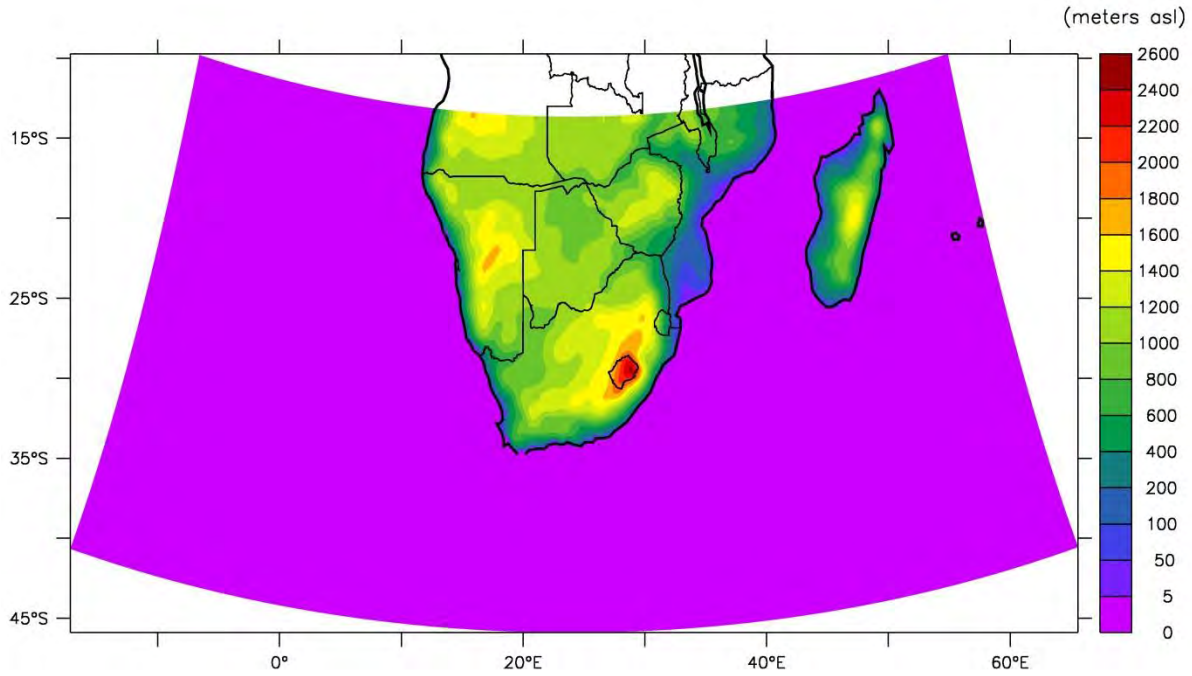

Figure 5 Simulation domain and terrain elevation as considered by both models.
The elevation is expressed in meters above sea level (asl).

3.3 Simulation of pollutants' trajectories

This study uses a lagrangian trajectory model to simulate the possible paths by which polluted air parcels over South Africa can be advected to Cape Town. To this end, the primary focus is on running trajectories from the industrial Highveld that covers parts of Gauteng and Mpumalanga provinces, the main source area of anthropogenic emissions in the country (Collett et al., 2000).

The lagrangian trajectory model was run using near-surface horizontal wind conditions (*u* and *v*) simulated by both RegCM and WRF, as initial conditions, with the assumption that there are no significant deviations in the vertical. Errors related to this assumption were minimized by running multiple trajectories. Thus, clusters of 36 air parcels were released daily (between January 1, 2001 and December 11, 2004; i.e. for 1441 days) from a 2.5° x 2.5° domain that covers the industrial Highveld of South Africa (Figure 6). The lagrangian model settings are such that, after one simulation day, the wind conditions at the new location are used to determine the next position, and so on until 20 days have been simulated. In other words, the path of each air parcel from the industrial Highveld was monitored for a maximum of 20 days. We considered 20 days because O_3 has an estimated mean lifetime of approximately 22 days in the troposphere (Stevenson et al., 2006).

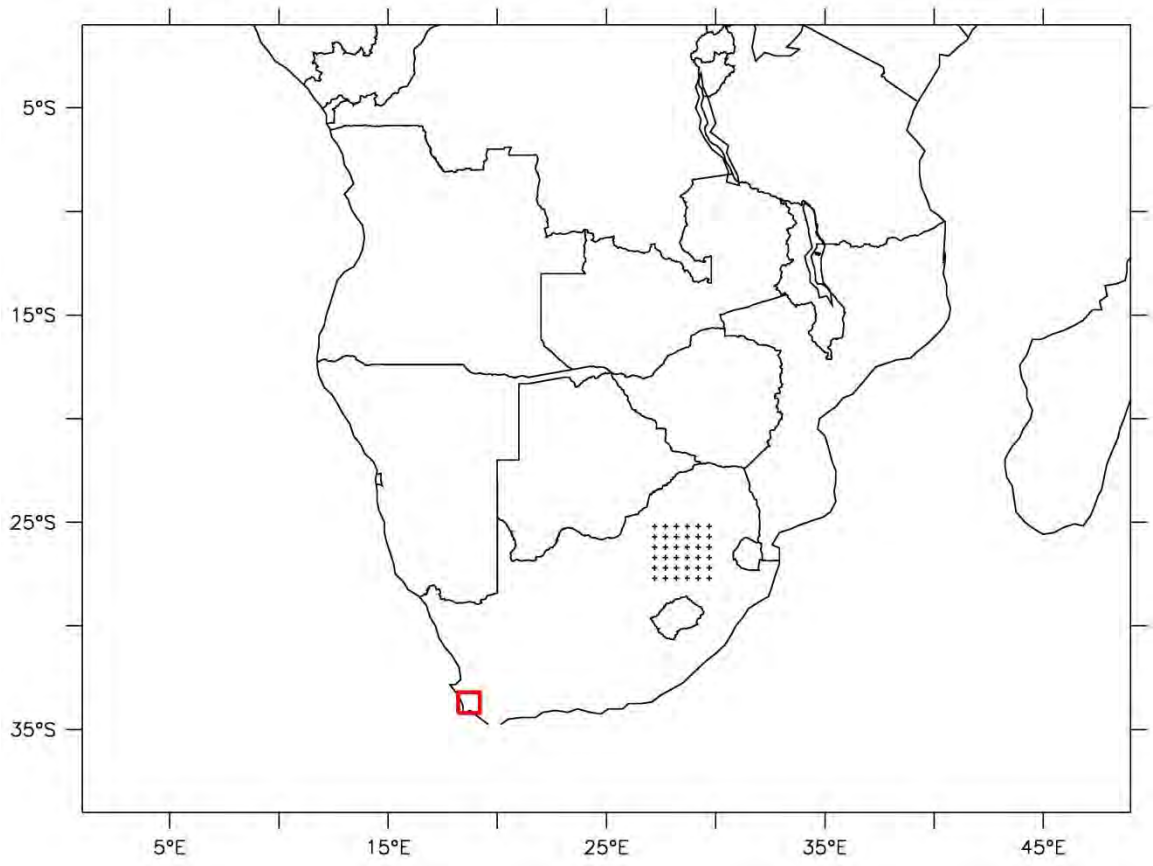

Figure 6 The location of the 6x6 point-array origin of clusters of lagrangian trajectories. The 36 point-origins are regularly spaced by 0.5° between 25.2°S-27.7°S and 27.2°E-29.7°E, a domain that covers the industrial Highveld of South Africa (i.e. parts of Gauteng and Mpumalanga provinces). The red square at the south-western tip of Africa shows the location of the Cape Town area.

Chapter 4: Results on the variation of ozone pollution in the Cape Town area

4.1 Diurnal variation

The diurnal variation of O_3 concentration in the Cape Town area varies from site to site. For instance, there is a clear difference between the diurnal cycle of O_3 concentration at Cape Point (remote background site) and at the sites close to the city centre (Figure 7a). The diurnal cycle of O_3 concentration at Cape Point features a single-mode pattern that peaks at 13h, reaching a maximum concentration of approximately 65 $\mu g/m^3$. Since there is no intense human activity near Cape Point, such a pattern suggests local production of O_3 primarily driven by sunlight and O_3 precursors from non-anthropogenic emissions. In contrast, the diurnal cycles of O_3 concentration at Molteno and Goodwood have an identical pattern with two peaks: a night-time peak (~30 $\mu g/m^3$) that occurs between 1h-5h, and a daytime peak (~45 $\mu g/m^3$) that occurs in the early afternoon between 12h-15h. However, Molteno experiences higher O_3 concentration than Goodwood, possibly because Molteno is located in the vicinity of the city centre where vehicle emissions are likely to be the highest in the Cape Town area. Moreover, the mountains surrounding Molteno may also constrain the dispersion of local pollutants, unlike Goodwood that is located on a flat environment.

Surprisingly, the O_3 concentration is higher at Cape Point (remote background site) than at Molteno (urban site) and Goodwood (sub-urban site) despite the presence of anthropogenic emissions of O_3 precursors in the city. A plausible

explanation is the presence of chemical sinks in urban and sub-urban environments of the Cape Town area. Indeed, measurements at the Goodwood station suggest that NO_x is a chemical sink of O_3 (Figure 7b), as the decline of O_3 concentration between 5h-8h and 18h-22h at Goodwood coincides with an increase of NO_x levels at that location. Another explanation is that there could be sources of major pollution upwind from Cape Point.

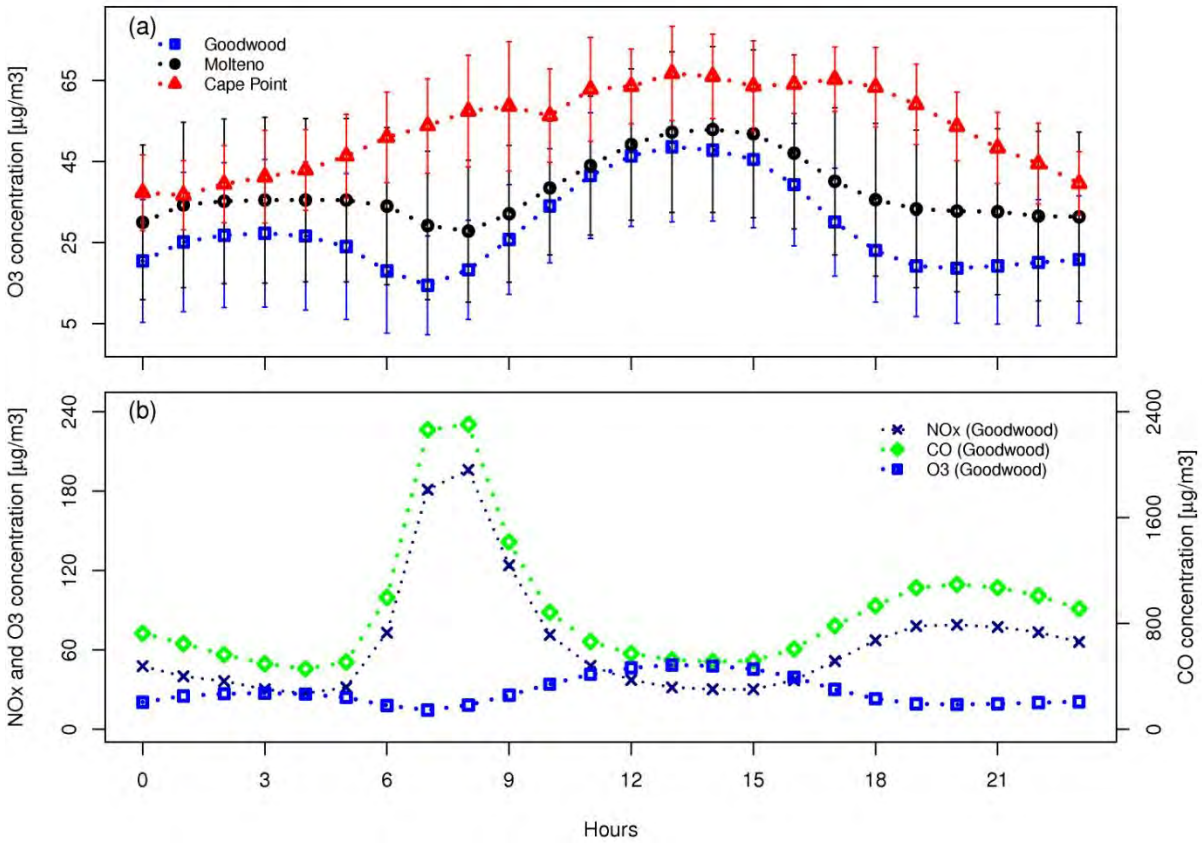

Figure 7 Diurnal variation of O_3 concentration at three locations in the Cape Town area. (a) Composite diurnal cycles of O_3 concentration at Cape Point, Molteno and Goodwood for the period 2001-2004. The vertical bars show the standard deviation (± 1σ) error. (b) Composite diurnal cycles of NO_x, CO and O_3 at Goodwood for the same period as in (a).

Figure 7b also suggests that the daytime O_3 peak at Goodwood is a result of the local emissions of NO_x and CO, six hours earlier. The early morning peaks of these O_3 precursors (at 8h), associated with traffic activity, contribute to the daytime O_3 peak (at 14h) through photochemical production of O_3. This relationship is evidenced by the lagged correlation between the diurnal cycle of O_3 and those of NO_x and CO at Goodwood (Figure 7b). Since the diurnal cycle of O_3 at Molteno features a similar pattern to that of Goodwood, the NO_x-O_3 and the CO-O_3 relationships described for Goodwood can be extended to Molteno, and probably to some other locations in the Cape Town area.

4.2 Seasonal variation

The concentration of ground-level O_3 in the Cape Town area also varies with the seasons. One should note that the seasonal cycle of O_3 concentration at Cape Point for our study period (2001-2004) is similar to that observed by Combrink et al. (1995) for 1988-1991. Most importantly, the O_3 concentration at that remote background is higher than that at the urban site (Molteno) and sub-urban site (Goodwood) (Figure 8a), and this difference is primarily due to the presence of chemical sinks in the city as discussed earlier for the diurnal variation. During summer, however, O_3 levels at Cape Point decrease to reach similar levels to those observed at the urban site (Molteno). Such a decline in summer is attributed to a destruction of O_3 molecules by photolysis (see Reaction R9). In addition, the strongest mean wind speeds at Cape Point occur during summer (Figure 8b) and may result in dispersion of air pollutants, leading to a reduction of O_3 concentration at this site.

In addition, the O_3 concentration is higher at Molteno than at Goodwood in all seasons (Figure 8a). A plausible explanation is that Molteno experiences weaker wind speeds (Figure 8b) caused by the mountains surrounding the site, inhibiting the horizontal mixing of local pollutants. Minimum O_3 concentration (~20 $\mu g/m^3$) at Goodwood occurs in winter and can be attributed to chemical removal by NO_x titration as it coincides with the maximum NO_x concentration at that site (see in Abiodun et al., 2013).

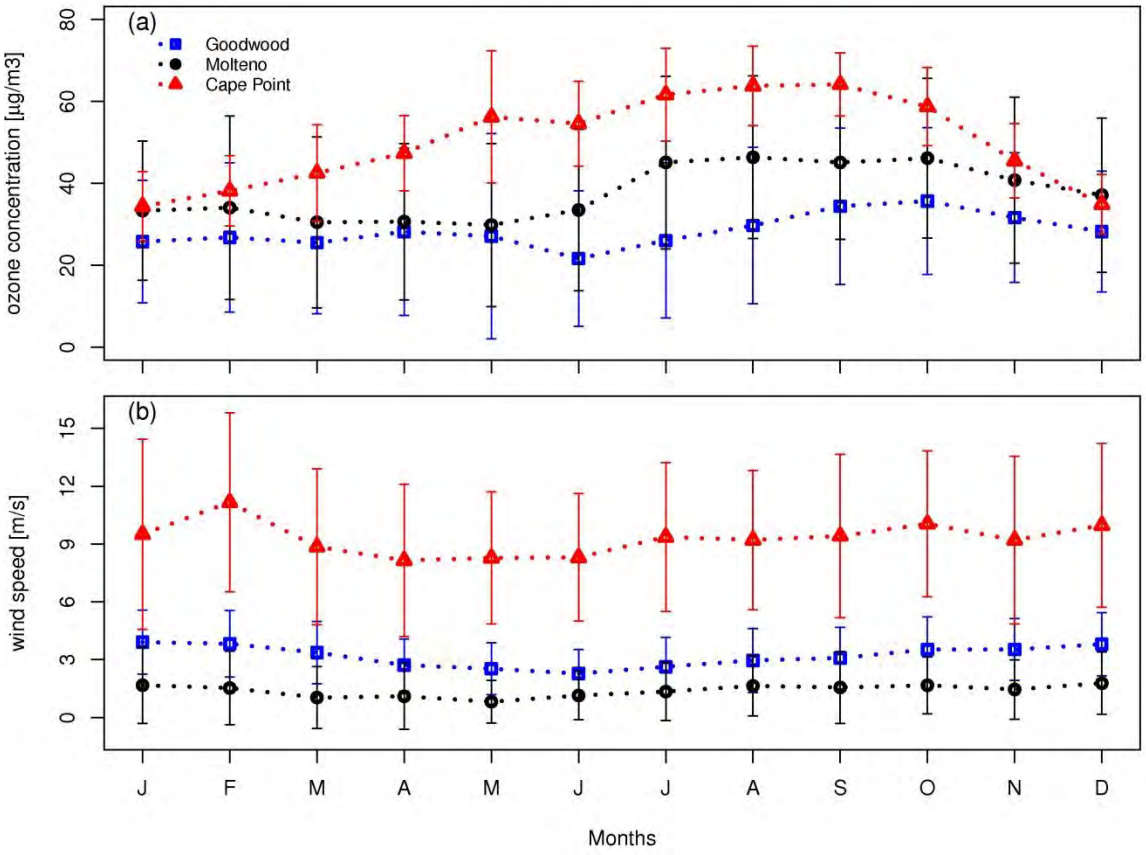

Figure 8 Seasonal variation of O_3 concentration at three locations in the Cape Town area. (a) Composite seasonal cycles of O_3 concentration at Cape Point, Molteno and Goodwood for the period 2001-2004. (b) Composite seasonal cycles of wind speed measured at the three sites for the same period as in (a). The vertical bars show the standard deviation (± 1σ) error.

The seasonal variation of O_3 levels at each site might also be influenced by the prevailing wind direction. At Cape Point, the lowest O_3 concentration in summer is associated with the prevailing strong southeasterly wind (Figure 9) that brings clean oceanic air to the site. This flow is identifiable as "*The Cape Doctor*", whose passage cleanses the atmosphere over most of the Cape Town area (City of Cape Town, 2005).

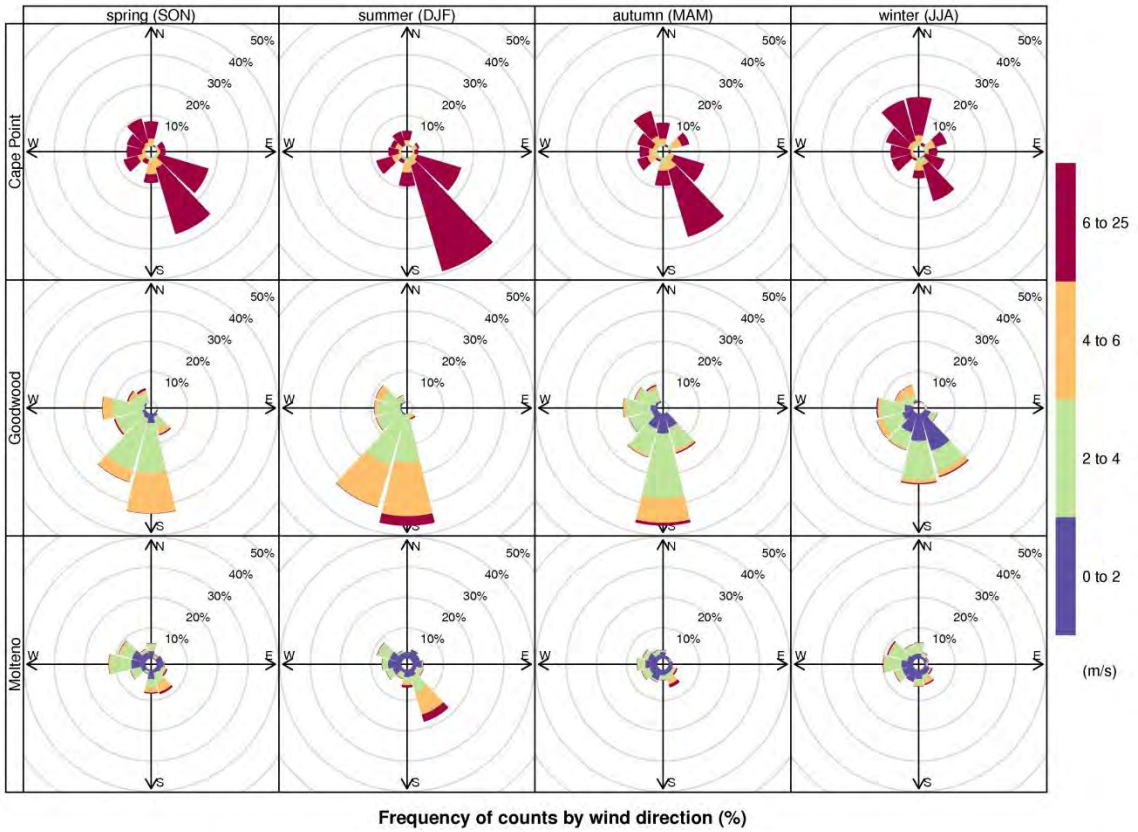

Figure 9 Seasonal wind roses at Cape Point, Goodwood and Molteno for 2001-2004.

In winter, when O_3 peaks at Cape Point, the prevailing wind regime at this site is from the north, suggesting input of pollutants from the city (Figure 9). At Goodwood, a prevailing southerly wind (Figure 9) suggests input of polluted air from the industries and townships in the south of the suburb. At Molteno, the highest O_3 levels in winter and spring can be associated with the calm wind conditions that favor the accumulation of pollutants, while the lowest levels in summer can be linked to the strong south-easterly flow (Figure 9).

4.3 Characterization of the October 12, 2003 extreme O_3 event

A noteworthy and rare extreme O_3 event occurred in the Cape Town area on the Sunday of October 12, 2003. On that day, levels of O_3 concentration at four locations (Molteno[9], Goodwood, Plattekloof[10] and Vissershok[11]) exceeded the local guideline threshold (98 $\mu g/m^3$ for 8 hourly averages) (City of Cape Town, 2013). According to the episode report by the local air quality services, the extreme O_3 event was due to extremely hot conditions that induced substantial photochemical production of O_3 and other secondary pollutants (City of Cape Town, 2013). In this study, available hourly data from Molteno and Goodwood were used to investigate the influence of local emissions and wind conditions on the occurrence of the extreme pollution event.

[9] Although the episode report by the City of Cape Town Air Quality Monitoring Section mentions Cape Town as one of the locations that experienced extreme O_3 levels on the October 12, 2003, the latter O_3 levels were measured at Molteno (Personal communication with Fazlin Waggie from the Air Quality Monitoring Section, City of Cape Town).
[10] Plattekloof is located to the northeast of Goodwood (~8 km).
[11] Vissershok is located to the north of Goodwood (~20 km).

We first analyze the variation of hourly O_3 concentrations at Molteno and Goodwood, between October 10, 2003 (00h) and October 14, 2004 (23h). At both sites, the five-day O_3 variation shows that more than 9 hourly readings (between 13h-21h) at Molteno exceeded 98 $\mu g/m^3$ on October 12, 2003, while only four exceeded the threshold at Goodwood (Figure 10a). The maximum concentration at both locations exceeded 150 $\mu g/m^3$ at 16h on that day.

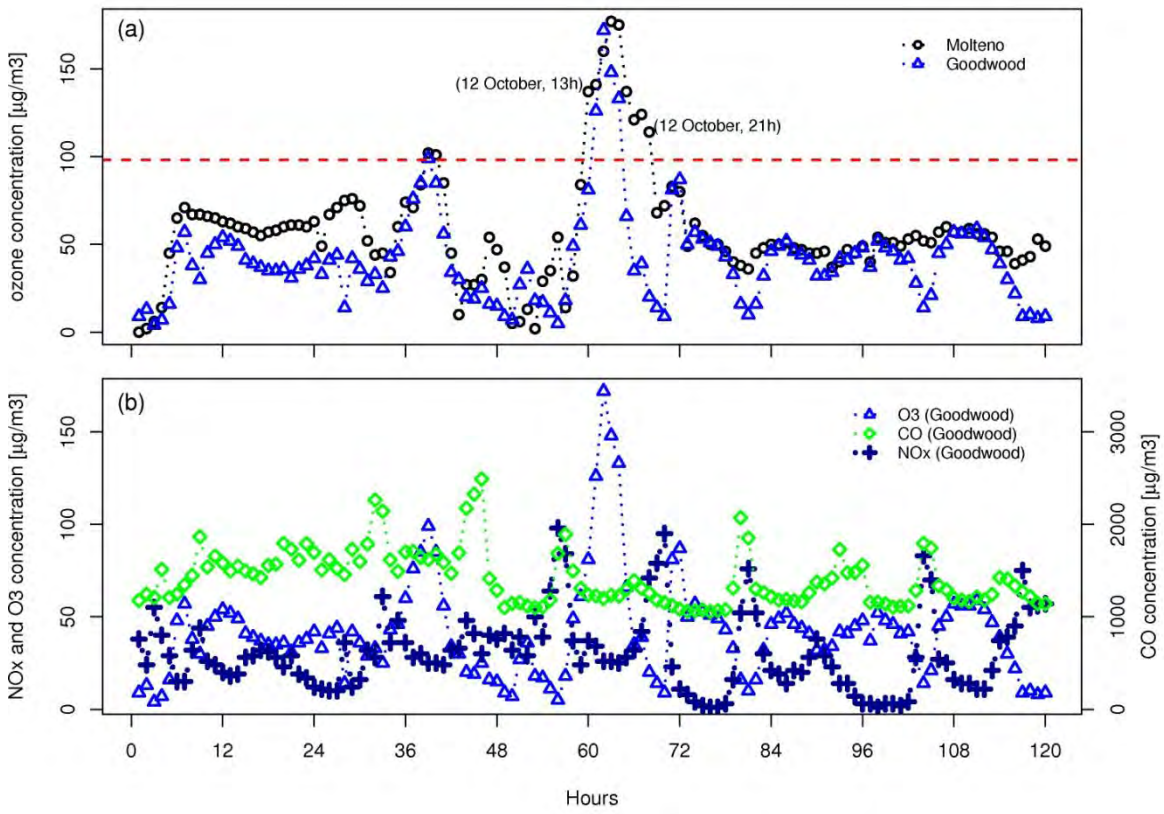

Figure 10 Hourly O_3 concentration from 10 to 12 October 2003 at Molteno and Goodwood. The five-day O_3 time-series starts at 00h (midnight) on October 10 and ends at 23h on October 12. (a) The horizontal dashed line indicates the standard threshold for an 8-hourly mean O_3 concentration (98 $\mu g/m^3$), as adopted by the City of Cape Town. (b) Variation of O_3, NO_x, and CO concentration at Goodwood for the same period as in (a).

Furthermore, the 120-hour time-series suggests that the extreme O_3 levels of October 12, 2003 were not due to aged O_3 pollution, but to a rapid increase in O_3 concentration during the morning of the same day (even if there were extreme O_3 levels during the afternoon (16h) of October 11, 2003 at both sites). It can also be seen that the extreme O_3 levels on October 12, 2003 did not persist to the next day (October 13, 2003).

Because both sites are located in environments where human activity occurs, it is likely that the extreme O_3 levels of October 12, 2003 were associated with anthropogenic emissions. By analyzing the variation of hourly NO_x and CO concentration at Goodwood, in comparison to those of O_3 at the same site, it is suggested that the O_3 extreme levels were caused by photochemical production (Figure 10b). This production might have occurred between the late morning (10h) and the late afternoon (16h), following the availability of O_3 precursors (i.e. NO_x and CO) in the early morning (8h-10h). However, it is surprising to see that NO_x levels at Goodwood on that Sunday morning (October 12, 2003) were higher (~100 $\mu g/m^3$) that those on other weekdays, suggesting that the extreme O_3 levels at that site were not associated with the usual commuting traffic around Goodwood. In addition, it is not clear whether NO_x and CO emissions were the principal drivers of the extreme O_3 levels on October 12, 2003 since levels of these O_3 precursors at Goodwood were also high on the mornings of the following two days (October 13-14, 2003), but associated with lower O_3 levels (~50 $\mu g/m^3$). Other factors that might have contributed to the extreme O_3 levels include meteorological conditions.

The wind conditions that prevailed between 9h-21h on October 12, 2003 at Goodwood show that the highest O_3 levels (>100 μg/m^3) were associated with calm conditions (~0.0 m/s wind speed), while the lowest O_3 levels (< 60 μg/m^3) were associated with stronger (>2 m/s) southerly winds (Figure 11). These conditions suggest that the O_3 that contributed to extreme pollution levels at Goodwood was locally produced, with possible additional pollutants advected from the south of the site (where there are informal settlements and small-scale industries). If this is the case, it is then probable that extreme O_3 levels at Plattekloof and Vissershok originated from Goodwood.

Unlike at Goodwood, the wind conditions that prevailed between 9h-21h on October 12, 2003 at Molteno suggest that the extreme O_3 levels at that site were associated with transported pollution (Figure 12). The figure suggests that the sources that contributed greatly to extreme O_3 levels were those located to the east of the site (probably in the southern suburbs) and those to the southeast (probably from residential areas in the vicinity of the station).

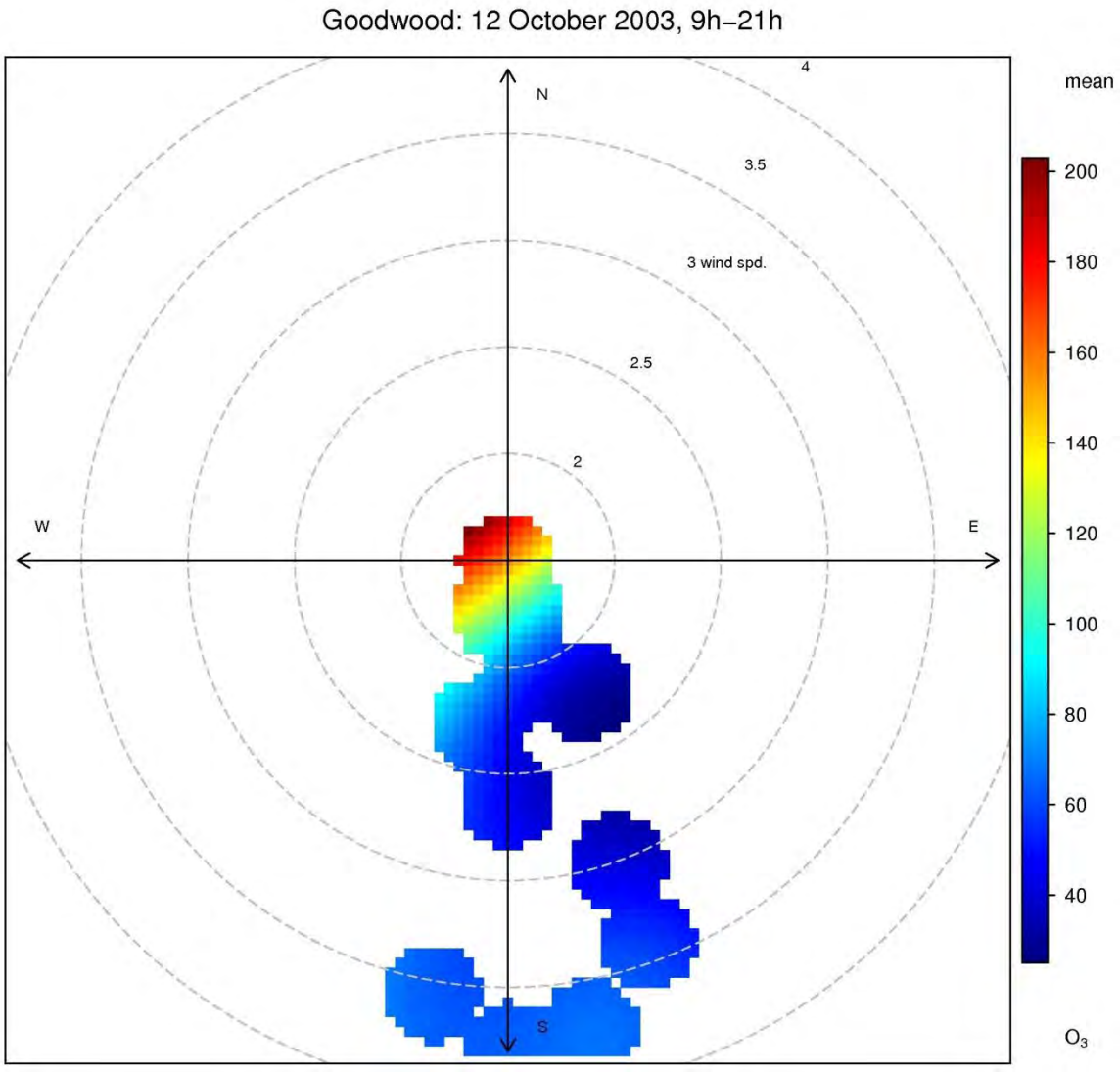

Figure 11 Polar plot of O_3 levels at Goodwood on October 12, 2003 between 9h-21h.
The plot shows the association between O_3 levels (in µg/m^3) and near-surface wind conditions at Goodwood during the indicated time. The wind speed (in m/s) is shown by the contour lines.

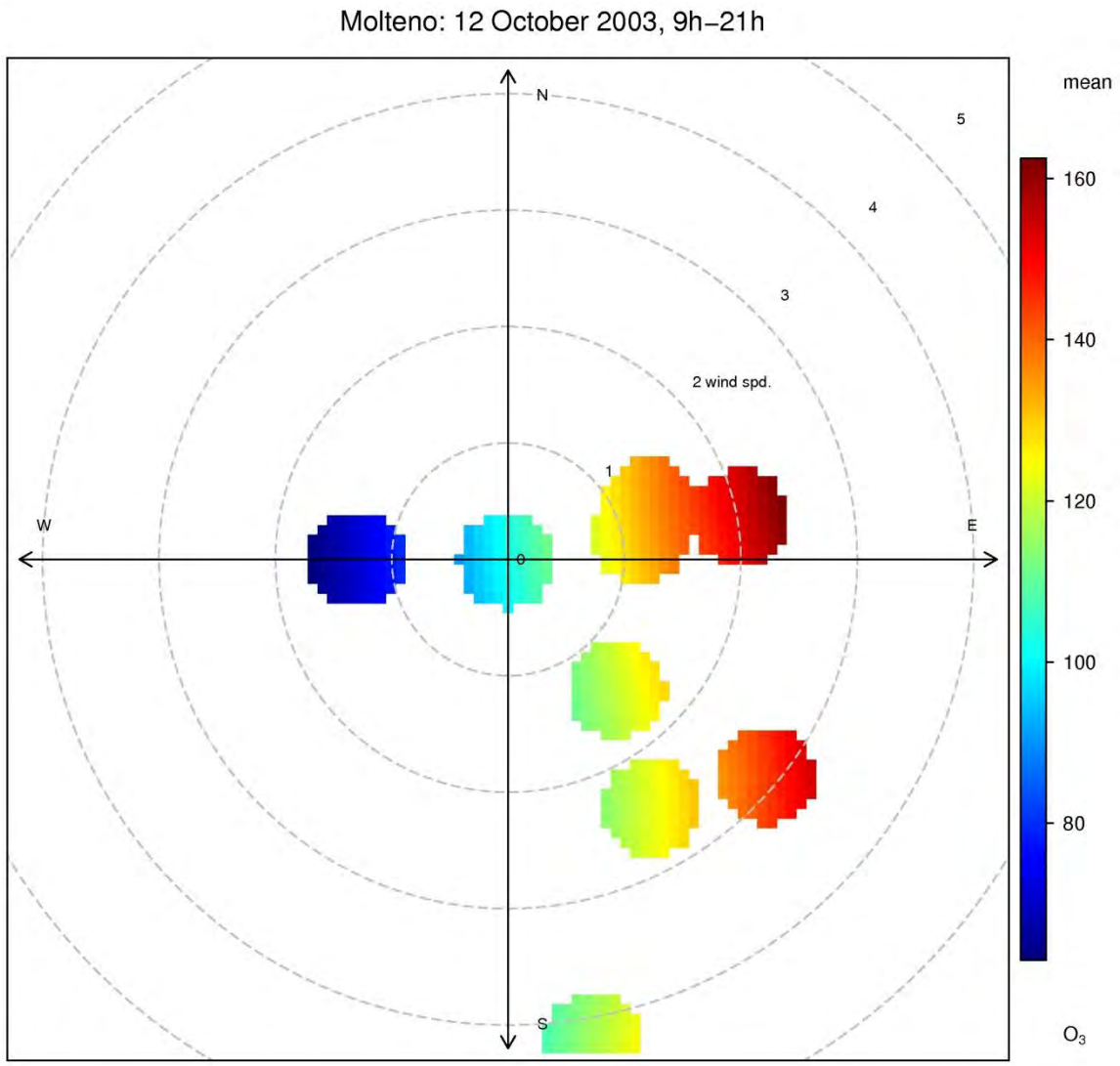

Figure 12 Polar plot of O_3 levels at Molteno on October 12, 2003 between 9h-21h.
The plot shows the association between O_3 levels (in µg/m^3) and near-surface wind conditions at Molteno during the indicated time. The wind speed (in m/s) is shown by the contour lines.

Chapter 5: Validation of the photochemical pollution simulated by RegCM and by WRF

Prior to the analysis of the photochemical pollution simulated by the RegCM and WRF models, the performance of each model in simulating the observed daily and seasonal variations of O_3 and NO_x concentrations as well as wind variables (speed and direction), was evaluated over the region delimited by 33°28'S to 34°55'S and 18°21'E to 18°55'E, representing the Cape Town area (Figure 6) and the region covering Molteno (33°93'S and 18°41'E), Goodwood (33°54'S and 18°33'E) and Cape Point (34°21'S and 18°29'E). Therefore, measurements from the three sites were averaged to represent the observed data over Cape Town. Measurements for air pollutants were normalized to allow a fair comparison with simulations.

Both models reproduce the daily wind speed over Cape Town well, as indicated by the positive correlations ($r \approx 0.6$) between the simulated and observed daily wind speed (Figure 13). In addition, both models simulate wind speed over Cape Town that compares well to the observed wind speed in terms of standard deviation ($0.5 < \underline{\sigma} < 1.0$). The comparable results from both models are mainly attributed to the initialization of the two models with the same meteorological data. However, the two models simulate dissimilar variation of photochemical pollutants over Cape Town. While nitrogen oxides (NO_x) simulated by RegCM do not correlate well with the observed NO_x ($r \approx 0.4$), simulated NO_x from WRF compare better to the observations ($r > 0.5$). Furthermore, NO_x simulations from WRF show a higher variability ($\underline{\sigma} \approx 2.0$) than those with RegCM, whose variability

(σ≈1.0) is comparable to the observations. Consequently (NO_x being an important precursor of O_3), the two models do not agree on the variation of simulated O_3 concentration over Cape Town. RegCM struggles to capture the daily mean concentration of O_3 over Cape Town as shown by the weak negative correlation (r≈-0.2). In addition, the simulated O_3 concentration has a higher standard deviation than the observed O_3 concentration (σ ≈ 1.5). WRF does better at simulating daily O_3 variation as r≈0.35 and σ ≈ 1.0.

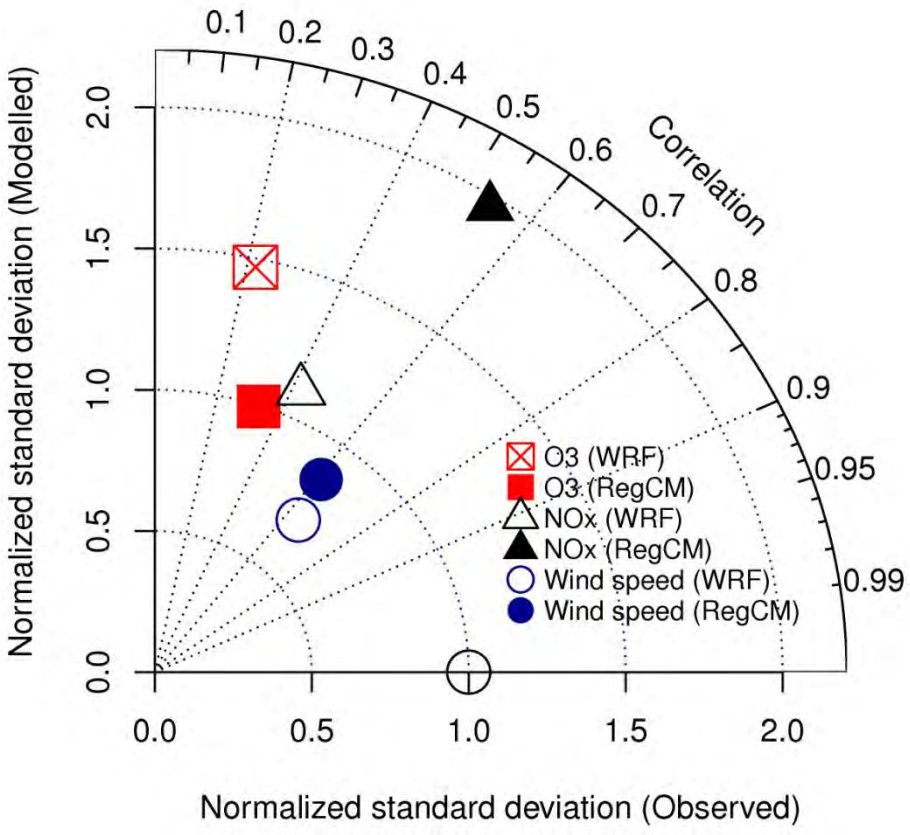

Figure 13 Taylor diagram for the simulated photochemical pollution over Cape Town.
In the diagram, the simulated concentration of photochemical pollutants (i.e. O_3 and NO_x) and wind speed over Cape Town are compared to the averaged pollutants and wind speed measured at air quality stations in the Cape Town area. The comparison is done using the coefficient of linear correlation (along the arc) and normalized standard deviation (along the axes). The crossed square shows negative correlation between simulated and measured O_3 over Cape Town.

The discrepancy between the observed and the simulated concentrations of air pollutants over Cape Town might also be due to the horizontal grid-resolution (35 km) at which the two models were run. In fact, a 35 km grid-resolution is suitable for regional atmospheric phenomena but is very coarse for local (city) scale studies. With such a resolution, the models cannot reproduce differences in the variation of O_3 observed at the various sites in the Cape Town area (Figures 7 and 8).

Again, due to the low spatial resolution of the simulations, both models have limited capacity to simulate all observed wind directions at the different sites in the Cape Town area (Figure 14 compared to Figure 9). Nevertheless, the models perform well in simulating the predominant south-easterly wind direction observed during spring, summer and autumn at Cape Point as well as during summer at Molteno. It is noteworthy that both models simulate comparable prevailing seasonal wind directions, probably due to the similar initial meteorological input data.

Furthermore, the seasonal variation of simulated concentration of O_3 over Cape Town is compared with observations (Figure 15a). Simulations by WRF demonstrate good skill at reproducing the seasonal variation of the averaged O_3 concentration over Cape Town. However, simulations with RegCM show a seasonal variation of O_3 that is very different to that of observed O_3 over Cape Town. While the measured O_3 concentration peaks between July and November, RegCM simulates a seasonal O_3 concentration maximum between March and April. The latter pattern is mainly driven by the seasonal cycle of the simulated

NO_x concentration which also peaks between March and April (Figure 15b). The simulations of photochemical pollution over Cape Town could be improved by initializing the chemistry with local emission inventories, preferably at higher resolution in both time and space.

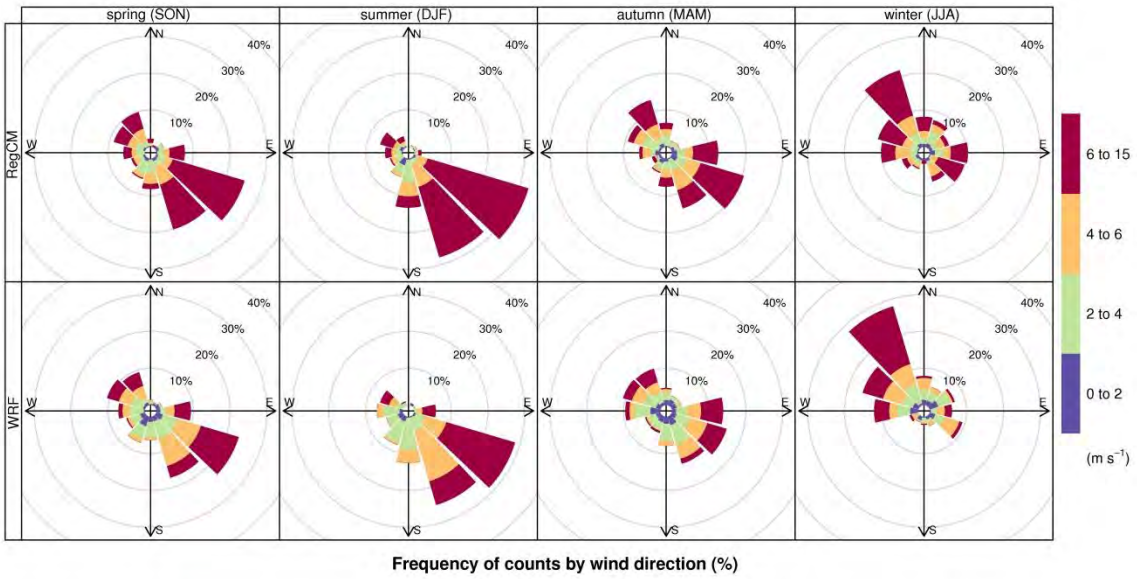

Figure 14 Seasonal roses for the simulated wind over Cape Town for 2001-2004.
The top row shows wind conditions over Cape Town as simulated by RegCM while the bottom row shows the wind characteristics as simulated by WRF.

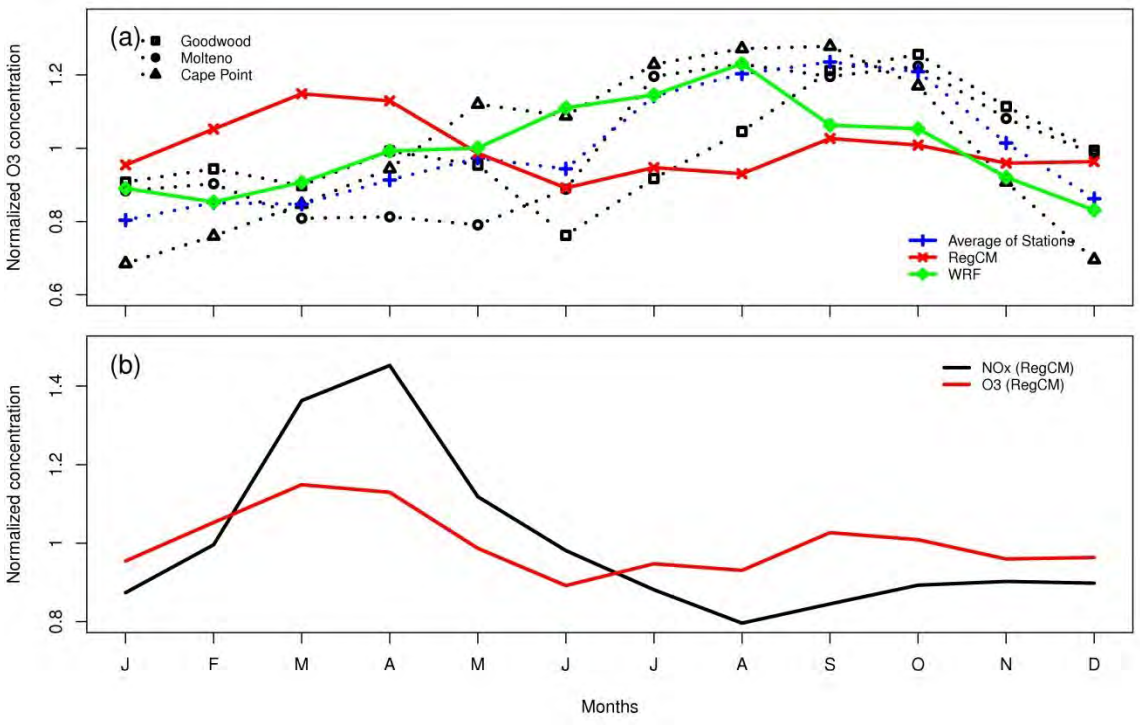

Figure 15 Seasonal variation of simulated O_3 levels over Cape Town for 2001-2004.
(a) Comparison of the simulated O_3 to that measured at Goodwood, Molteno and Cape Point.
(b) Comparison of the seasonal O_3 and NO_x cycles over Cape Town as simulated by RegCM.

Chapter 6: Results on the regional transport of ozone pollution over Cape Town

6.1 Seasonal distribution of ozone precursors over South Africa

In this chapter, we consider the pollutants' concentration in the lower troposphere (near surface), which corresponds to the lowest grid of the models. Although WRF captures the variation of O_3 concentration over Cape Town well, the model simulates an unreliable spatial distribution of O_3 over southern Africa (Figure 16). In fact, between April and September, unusual maxima levels of O_3 concentration are simulated over the Atlantic and Indian Oceans adjacent to South Africa. It is not clear whether these high O_3 levels are due to emissions transported from the continent or if there are errors in the boundary conditions. Nonetheless, the simulated O_3 precursors suggest a cause to that problem. Indeed, while WRF simulates a reliable distribution of some precursors (such as NO_x and xylenes) (Figures 17 and 20), simulated concentrations of some other chemicals (for instance, CO and ethylene) are substantial over the marine areas adjacent to South Africa (Figures 18 and 19). Another odd result found in the WRF outputs is a semi-permanent O_3 hot-spot simulated over Lesotho, higher than anywhere else on the subcontinent between October and March. Therefore, the distribution of O_3 as simulated by WRF is judged to be too unreliable for use in studying its regional-scale transport. On the other hand, the simulations by RegCM provide a more reliable spatial distribution of the concentration of O_3 and its precursors over South Africa. Hence, most results presented in this chapter are based on RegCM simulations over the subcontinent.

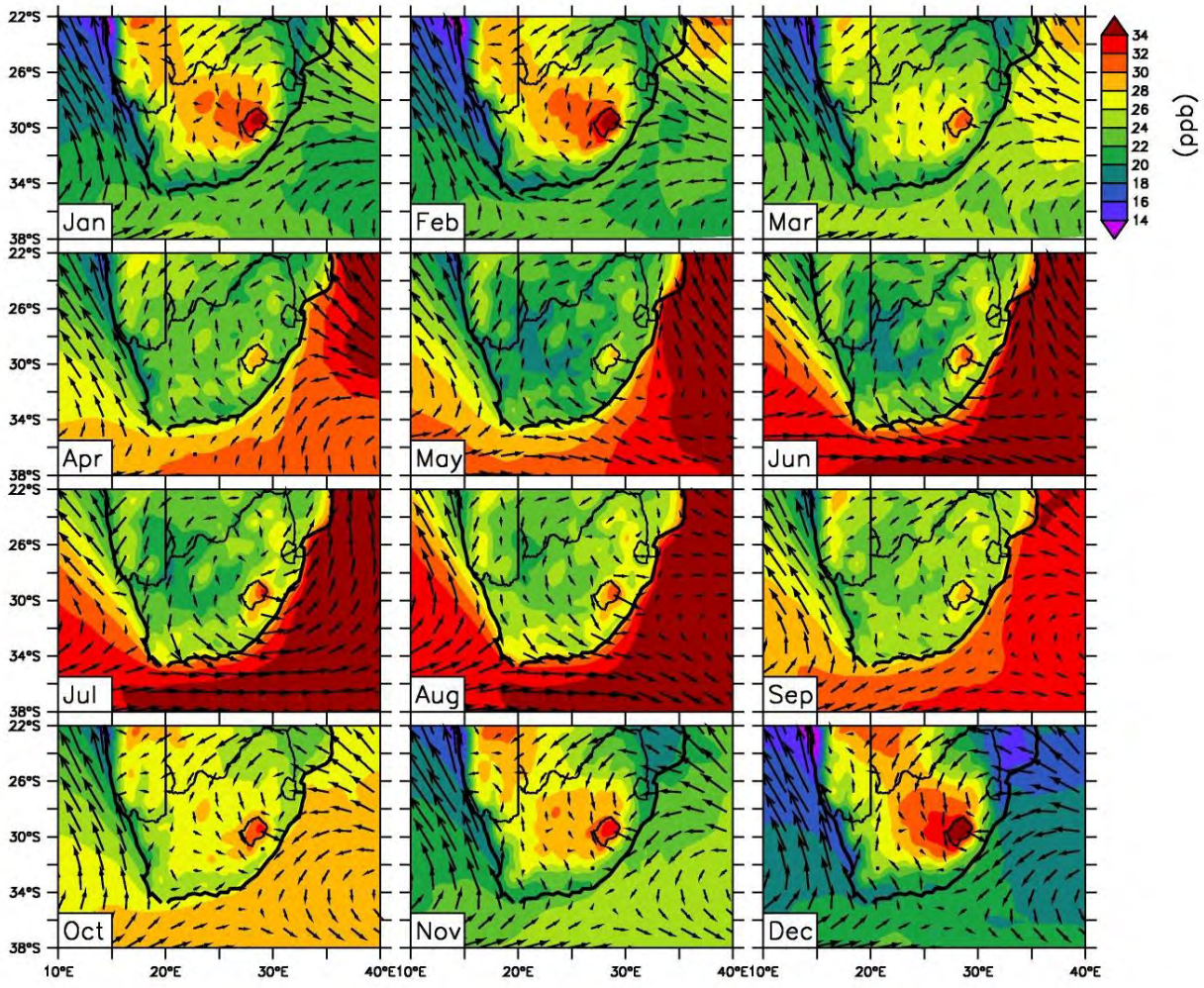

Figure 16 Seasonal distribution of O_3 over South Africa as simulated by WRF.
The figure also shows the seasonal variation of the simulated wind field over South Africa.

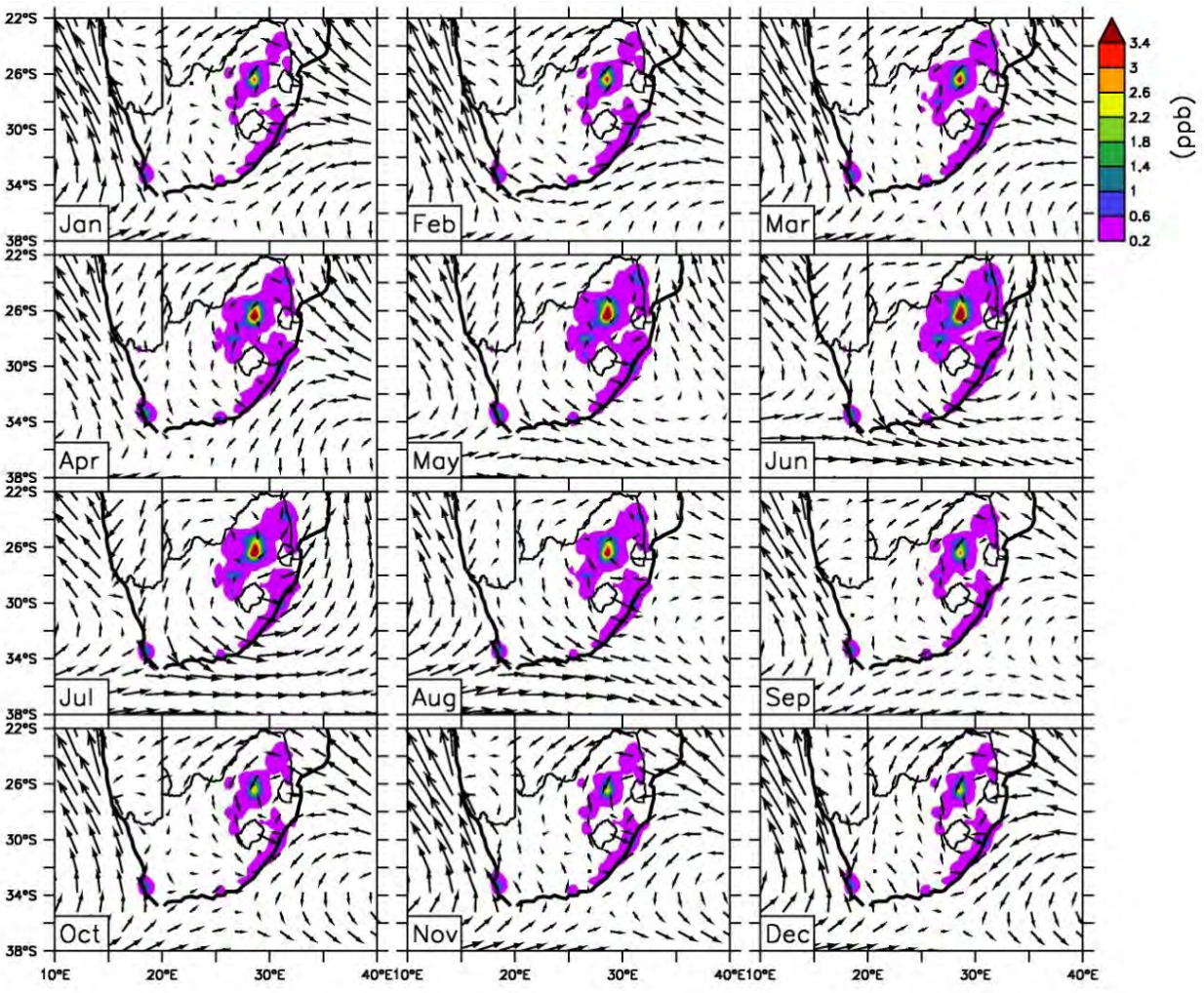

Figure 17 Seasonal distribution of NO_x over South Africa as simulated by WRF.
The figure also shows the seasonal variation of the simulated wind field over South Africa.

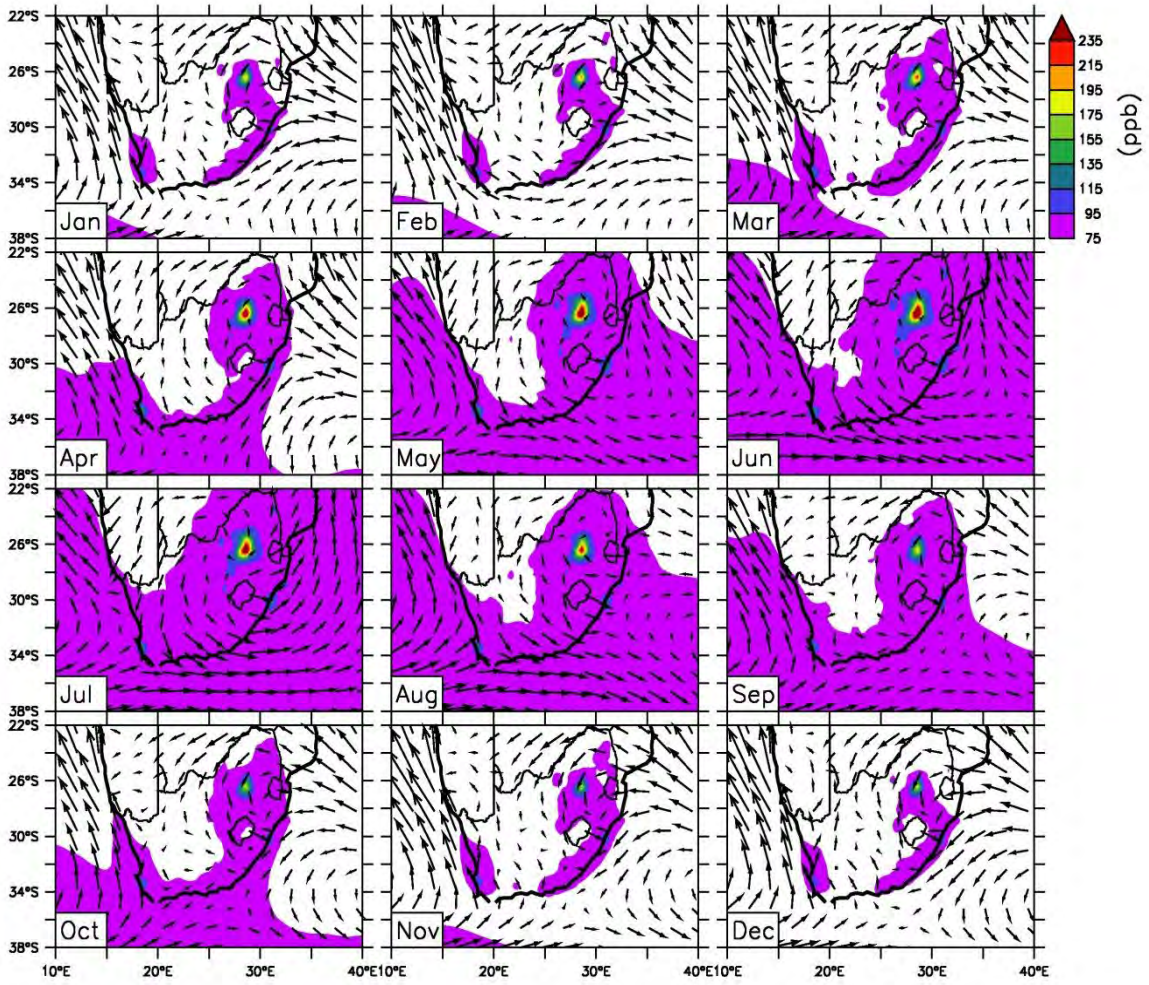

Figure 18 Seasonal distribution of CO over South Africa as simulated by WRF.
The figure also shows the seasonal variation of the simulated wind field over South Africa.

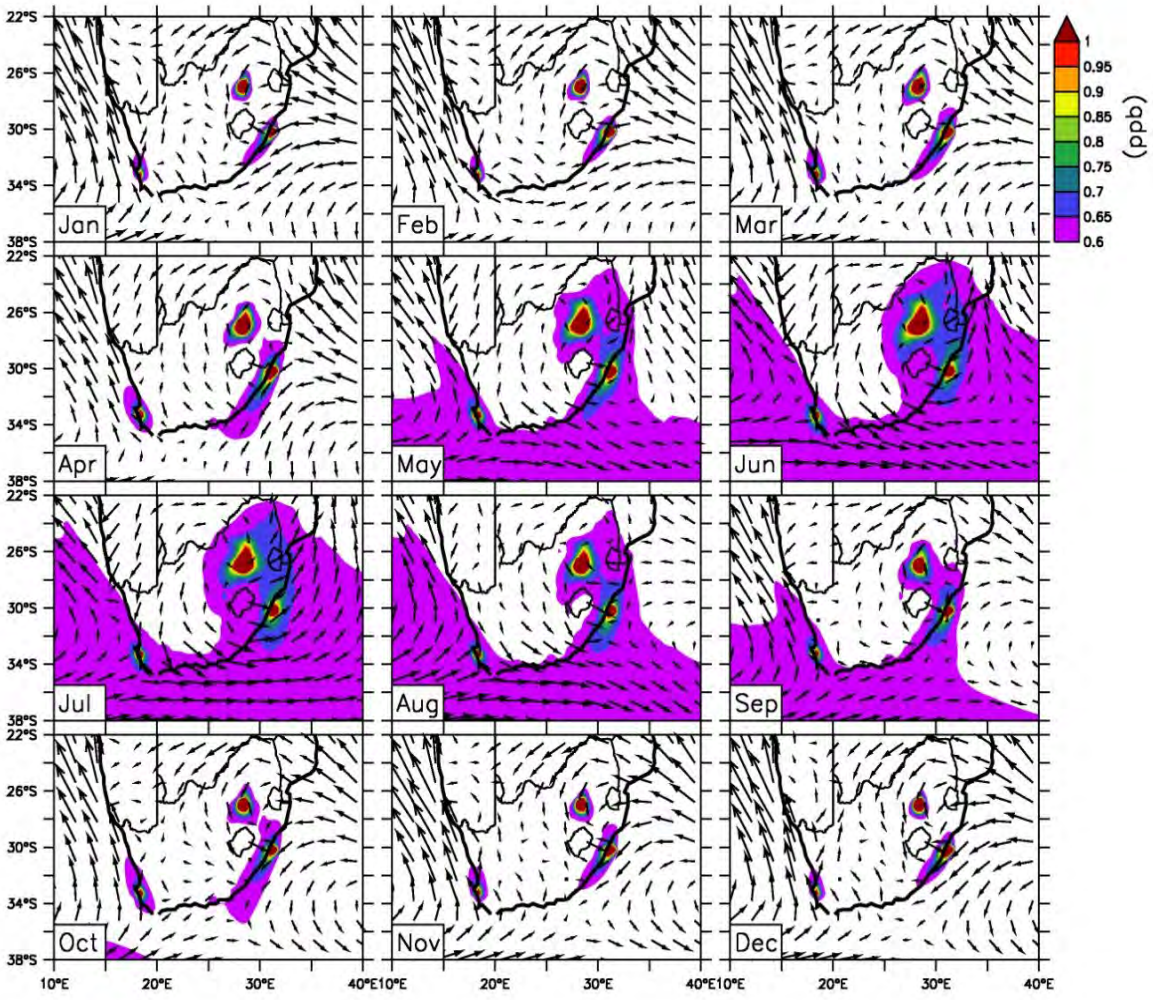

Figure 19 Seasonal distribution of ethylene over South Africa as simulated by WRF. The figure also shows the seasonal variation of the simulated wind field over South Africa.

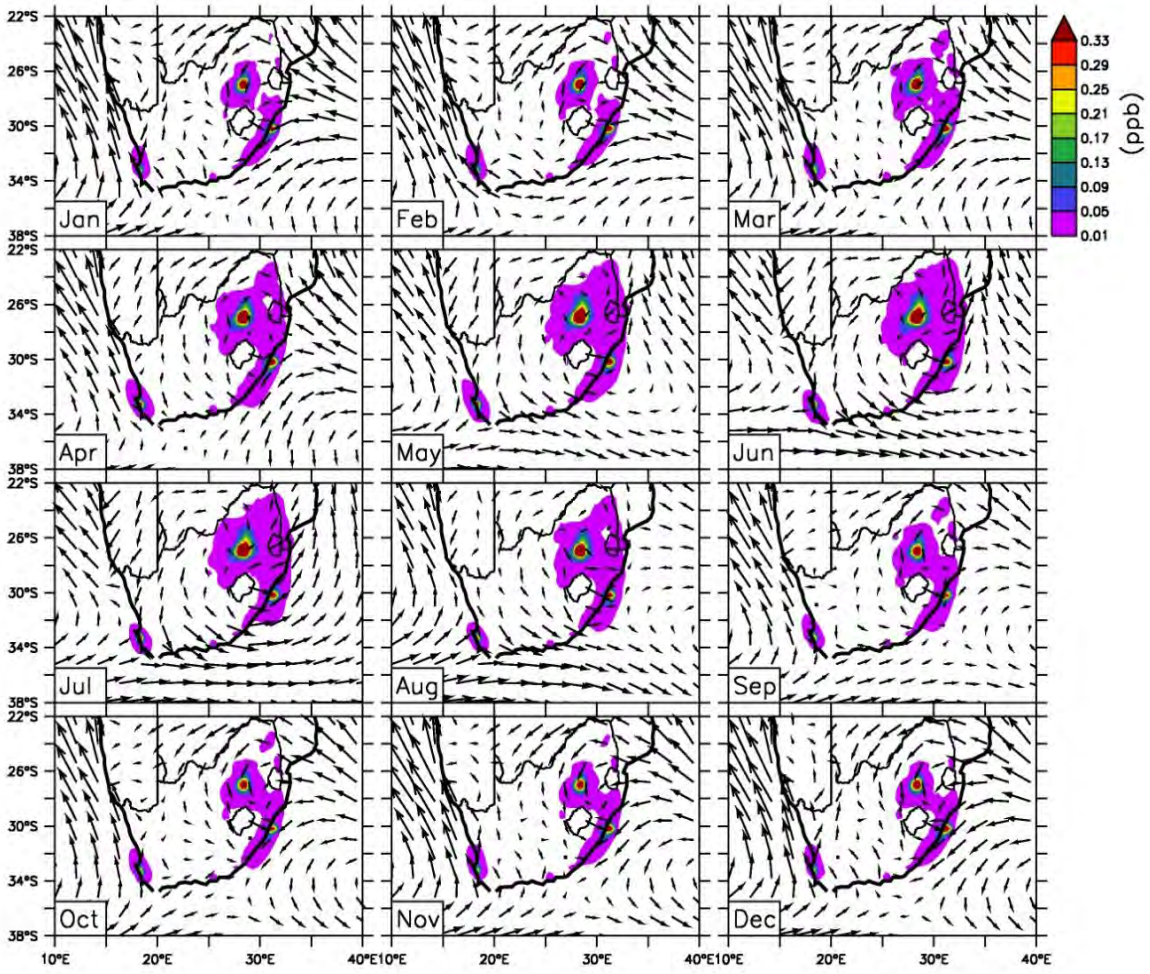

Figure 20 Seasonal distribution of xylenes over South Africa as simulated by WRF. The figure also shows the seasonal variation of the simulated wind field over South Africa.

Using simulations by RegCM for the period 2001-2004, we analyze the seasonal distribution of nitrogen oxides (NO_x), carbon monoxide (CO), ethylene and xylenes over South Africa. Their spatial distribution helps understanding the potential sources of O_3 in South Africa and its regional-scale transport. The simulations show that, throughout the year, the aforementioned O_3 precursors are mostly concentrated over the eastern side of South Africa (from 25°E eastwards) (Figures 21-24). Permanent hot-spots of these O_3 precursors are simulated over the industrial Highveld, where the country's dominant mining exploitation (Mpumalanga) and urban infrastructure (Gauteng) are located. However, comparable NO_x levels are simulated on the border of South Africa and Botswana and in the south of Lesotho (Figure 21). These two hot-spots are also found in the NO_x emission data used to initialize the photochemistry in RegCM (Figure 3a). Besides the maxima O_3 levels over the industrial Highveld, substantial levels of O_3 precursors are simulated over major cities of South Africa, such as Durban on the south-east coast and Cape Town on the south-west coast. This result is in agreement with the emission inputs (Figure 3), suggesting that urban areas of South Africa are potential sources of O_3. Therefore, apart from O_3 that might be transported to Cape Town, there is O_3 that is primarily produced from local emissions.

Other noteworthy features are simulated between July and October, for CO (Figure 22). High levels of CO are simulated to be widespread over tropical southern Africa. This seasonal pattern is attributed to biomass burning events that are frequent in spring, releasing CO and other various O_3 precursors from

fire emissions. As it will be shown later, the increase in O_3 precursors during that season contributes to increasing O_3 concentration over southern Africa.

Between August and September, the prevailing wind conditions suggest that pollutants from eastern South Africa are transported towards the east coast, resulting in extreme pollution levels on the coast (Figures 21-24). The pollutants accumulate along the coastal region by the influence of prevailing easterly winds from the Indian Ocean, preventing an effective transfer of the pollution to the atmosphere over the ocean. This result is consistent with previous studies based on measurements (e.g. Stein et al., 2003), in which high levels of pollutants and haze conditions along the eastern coastal region of southern Africa were attributed to meteorological conditions (and not to local emissions). This simulated phenomenon will be discussed further for the regional distribution of O_3.

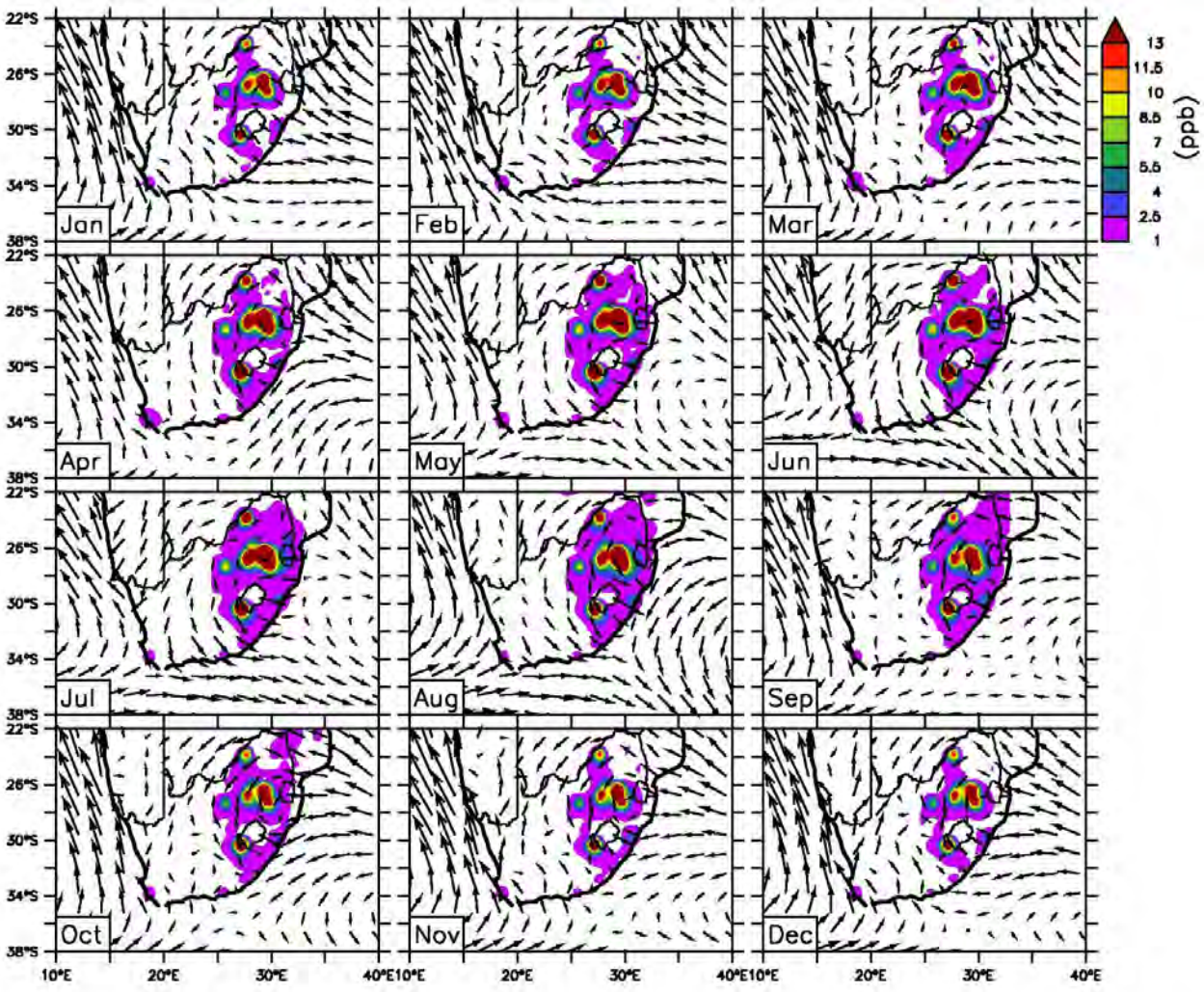

Figure 21 Seasonal distribution of NO_x over South Africa as simulated by RegCM.
The figure also shows the seasonal variation of the simulated wind field over South Africa.

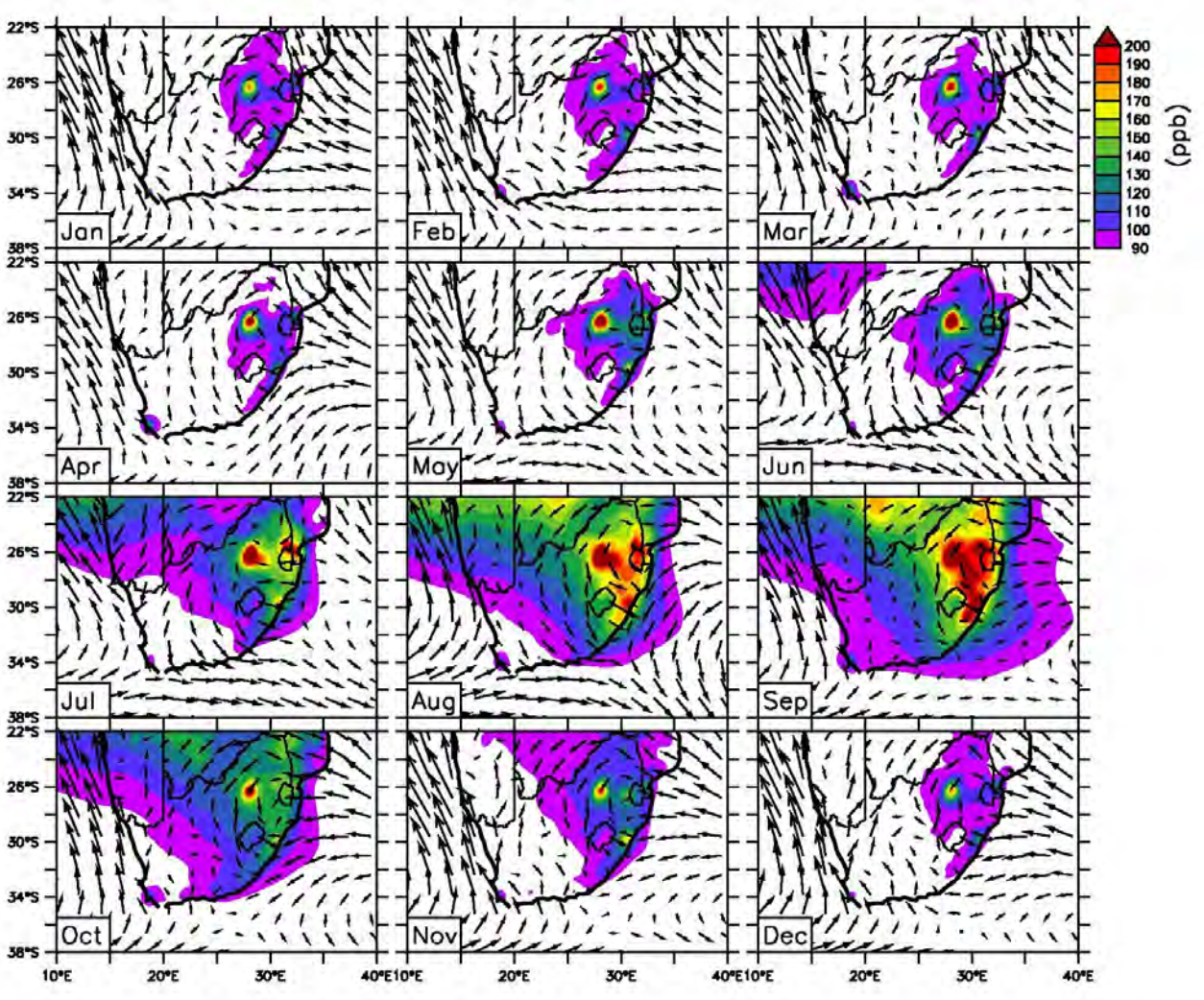

Figure 22 Seasonal distribution of CO over South Africa as simulated by RegCM.
The figure also shows the seasonal variation of the simulated wind field over South Africa.

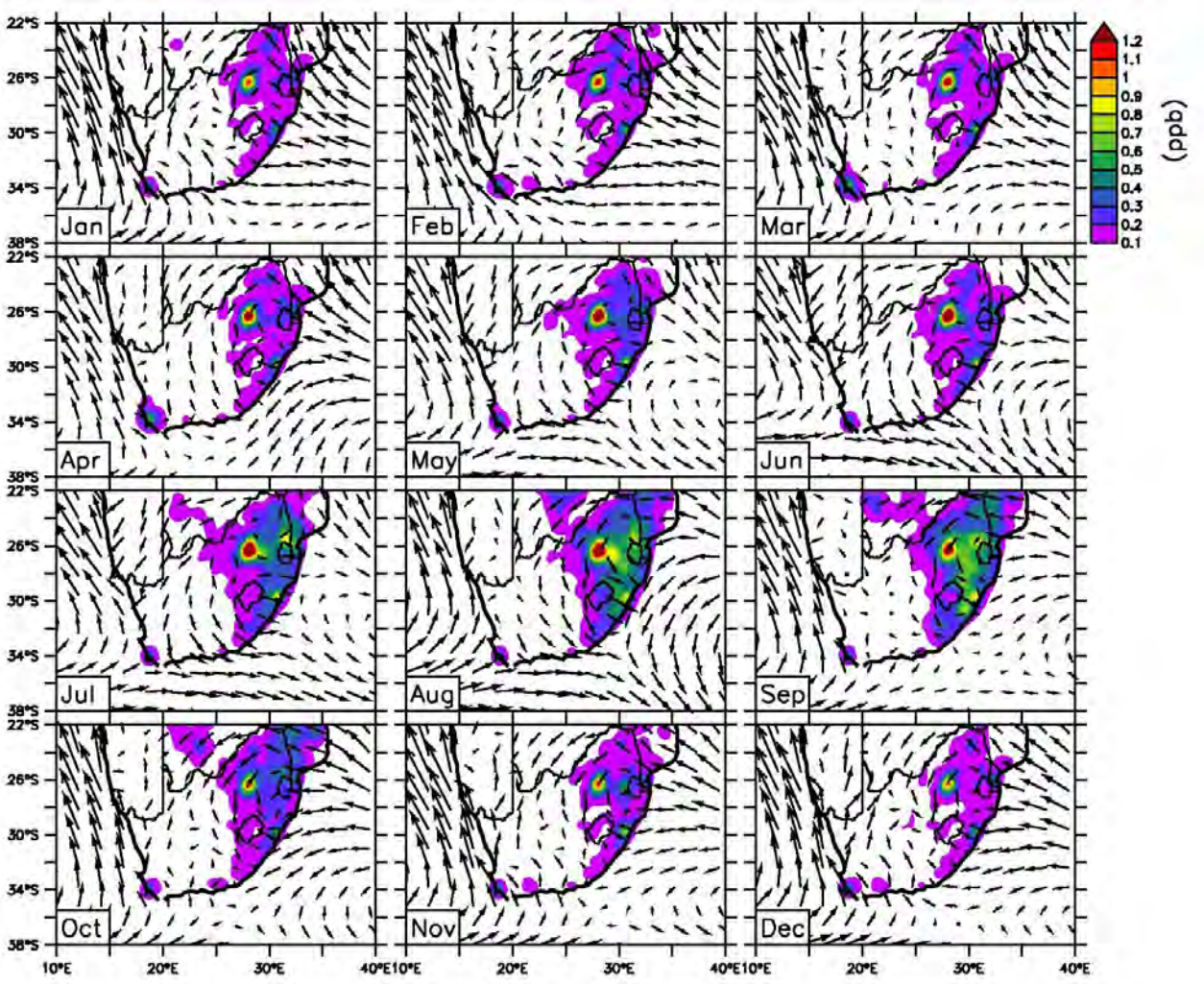

Figure 23 Seasonal distribution of ethylene over South Africa as simulated by RegCM. The figure also shows the seasonal variation of the simulated wind field over South Africa.

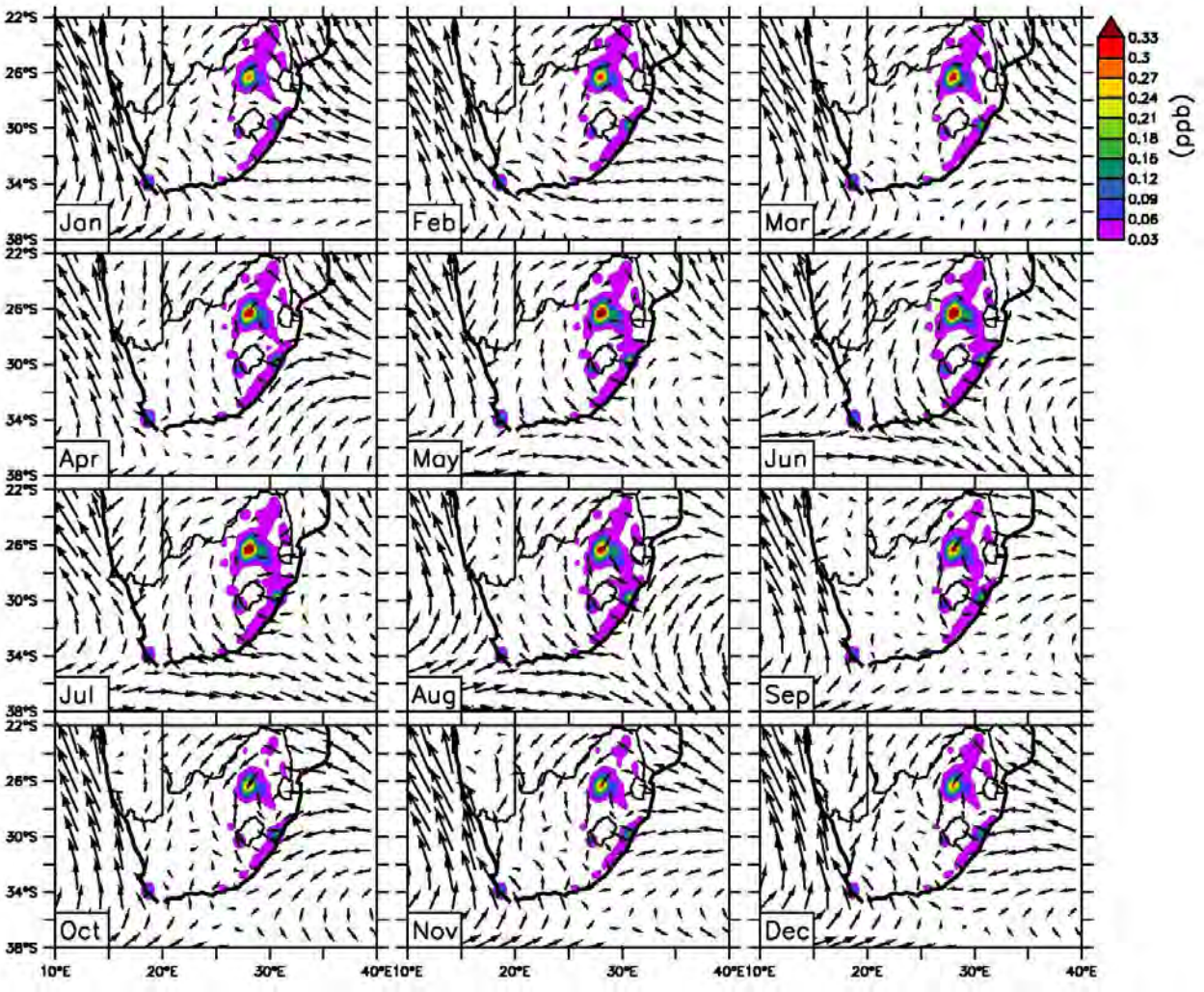

Figure 24 Seasonal distribution of xylenes over South Africa as simulated by RegCM. The figure also shows the seasonal variation of the simulated wind field over South Africa.

6.2. Seasonal distribution of tropospheric ozone over South Africa

We also analyze the seasonal distribution of O_3 over South Africa, as simulated by RegCM, for the period 2001-2004 (Figure 25). The model simulates a semi-permanent hot-spot of O_3 concentration (>25 ppb) over the north-eastern Highveld of South Africa, consistent with the emission rates over that region (Figure 3). Both these emission rates and the O_3 hot-spot suggest that the north-eastern Highveld region (the industrial Highveld), is an area where O_3 is produced in substantial quantities throughout the year. However, the O_3 hot-spot is more intense and covers a wider area between July and September, when it extends from the Highveld to the eastern coast of the country. The simulated wind suggests that, during that season, O_3 pollution from the industrial Highveld is transported towards the east and southeast coasts. Then, the pollution gets trapped along the coast by the confluence of the westerly winds from the continent and easterly winds from the Indian Ocean, resulting in an accumulation of O_3 along the coastline (Figure 25). In other words, this O_3 hot-spot over the east coast of South Africa is caused by meteorological conditions that favor the accumulation of pollutants, in agreement with Stein et al. (2003), who associated seasonal haze conditions (between August-September) over the same region with stagnant atmospheric conditions (for instance, the formation of an atmospheric col or the presence of weak high-pressure systems).

The simulated O_3 concentration anomalies (with respect to the annual O_3 mean concentration) show that, between August and October, O_3 concentration increases (positive anomalies) over parts of Namibia, Botswana and Zimbabwe,

as well as parts of the Indian and Atlantic Oceans (Figure 26). These positive anomalies are mainly attributed to substantial O_3 production following the biomass burning emissions that prevail over tropical southern Africa during these months (Thompson et al., 1996a). Such regional biomass burnings release chemical compounds that include O_3 precursors such as CO, hydrocarbons and NO_x, leading to high O_3 levels and sometimes to O_3 maxima over most of southern Africa (Thompson et al., 1996a).

During other months, lower emissions from biomass burning together with atmospheric conditions are responsible for the negative anomalies of O_3 over north-eastern South Africa. Between November and April, inflows from the Indian Ocean penetrate inland and, dilute the atmosphere over the north-eastern region of the country, while transferring some pollutants towards the south and southwest. Between February and April, Cape Town and the south-western coast of South Africa experience positive anomalies especially in March and April. However, these positive anomalies are lower than those simulated over the north-eastern region of the country between July and September.

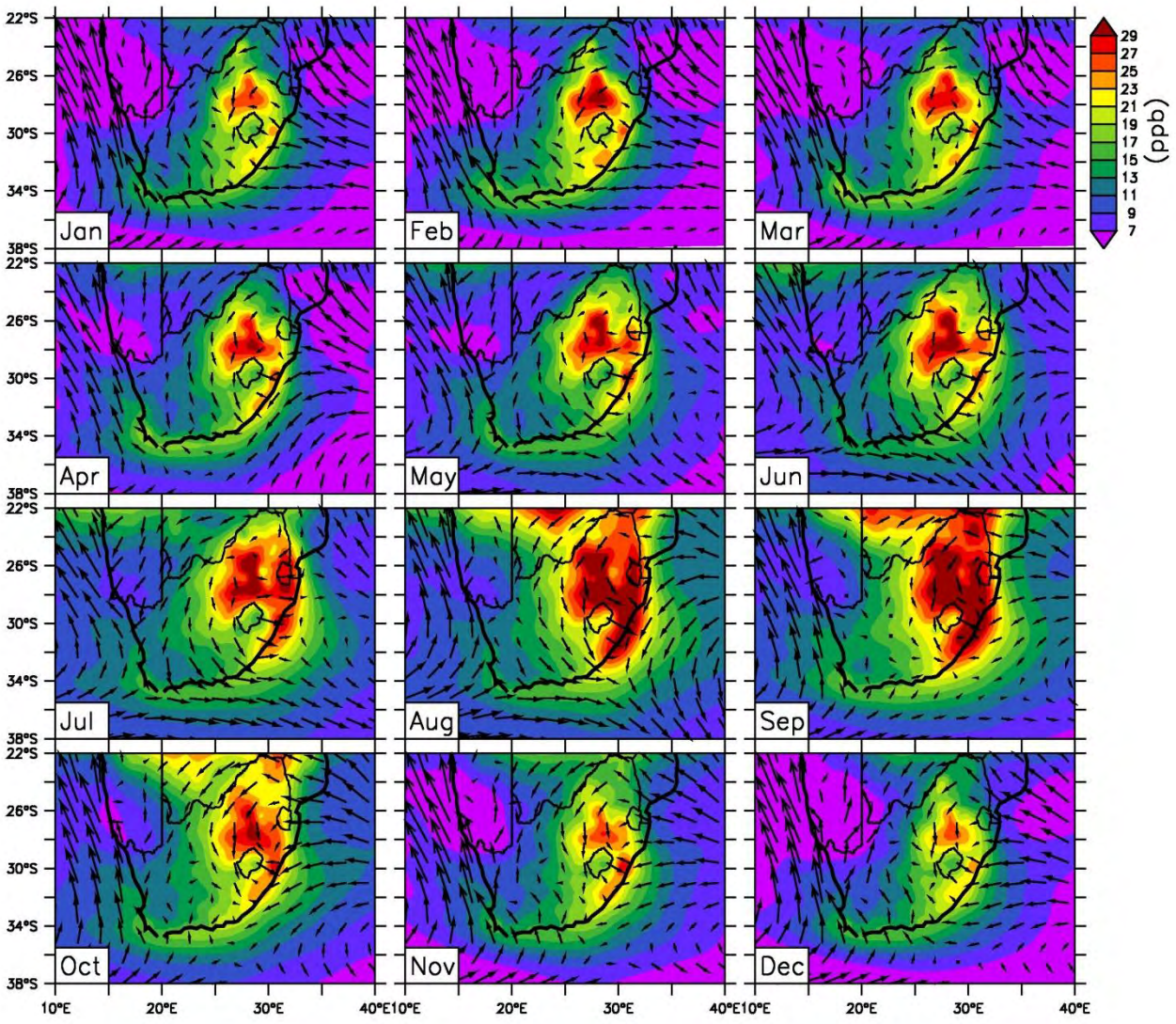

Figure 25 Seasonal distribution of O_3 over South Africa as simulated by RegCM.
The figure also shows the seasonal variation of the simulated wind field over South Africa.

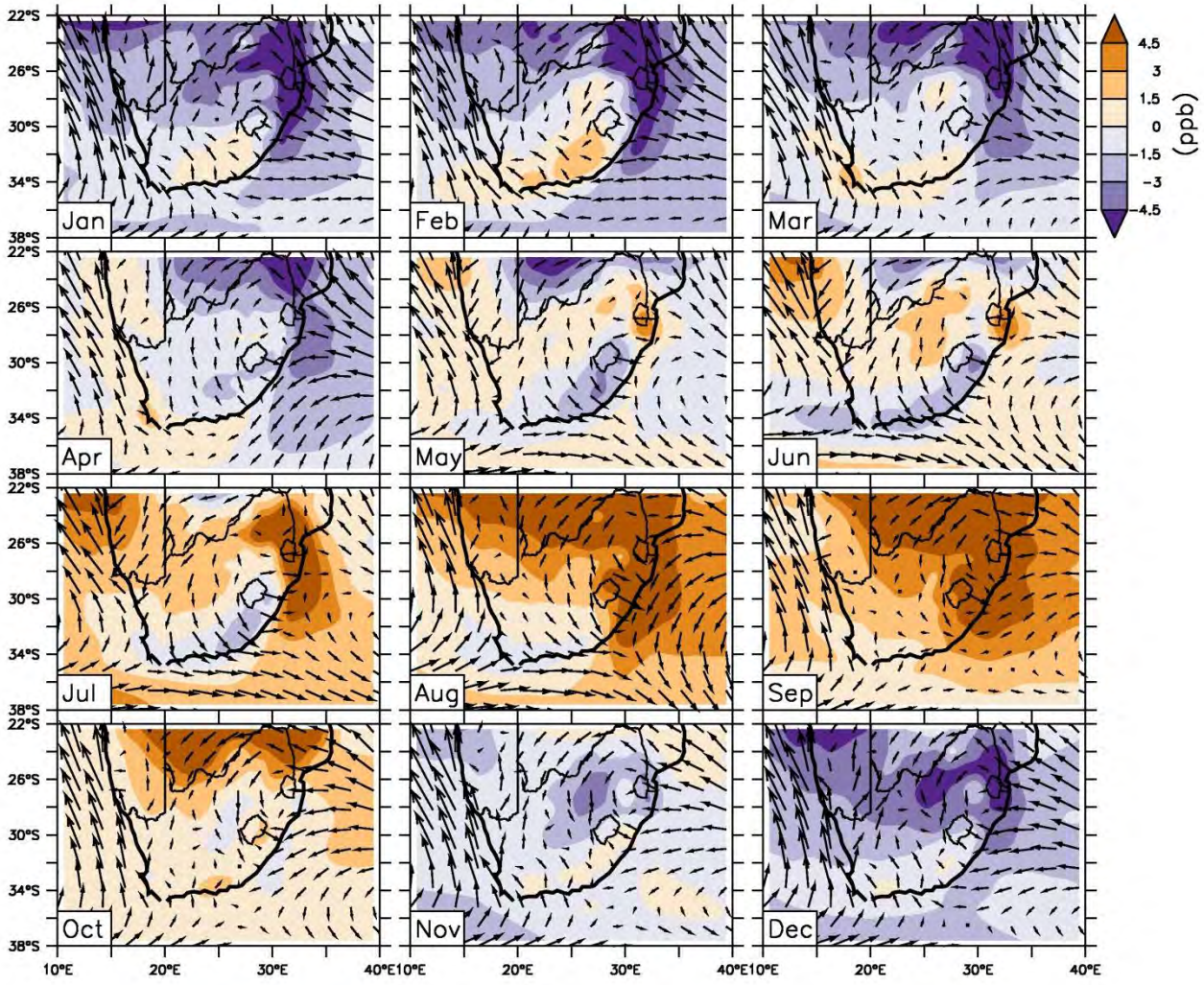

Figure 26 Seasonal O_3 concentration anomalies over South Africa as simulated by RegCM. The O_3 anomalies are calculated with respect to the annual O_3 mean. The figure also shows the seasonal variation of the simulated wind field over South Africa.

6.3 Regional transport and extreme ozone pollution over Cape Town

As part of this study, we investigate the influence of the regional-scale transport of O_3 pollution on air quality in Cape Town. Based on the four-year simulations by RegCM, we identify days with extreme O_3 levels over the Cape Town area (see on Figure 6) as days on which the simulated daily O_3 concentration exceeds the the 99th percentile value (27 ppb).

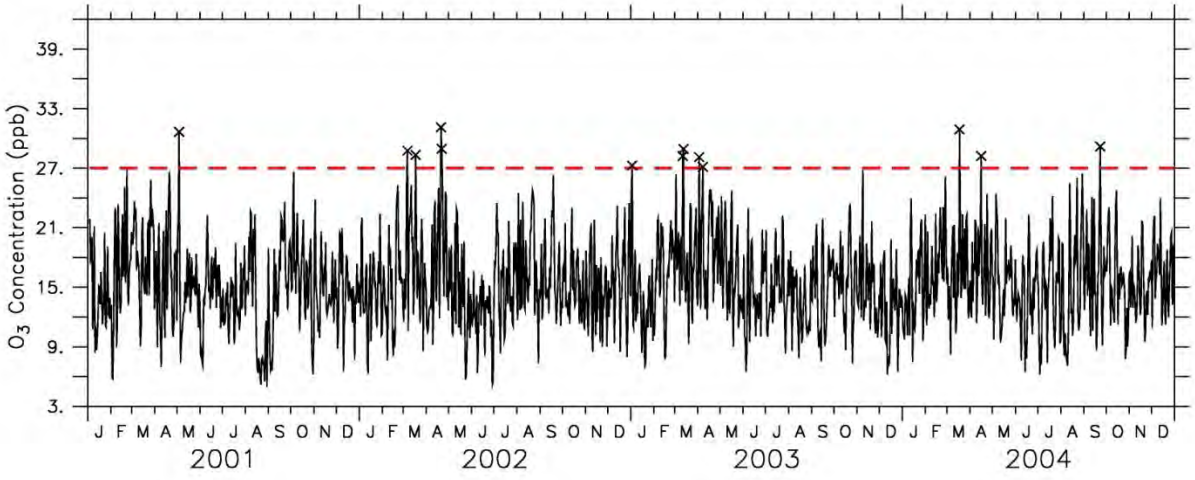

Figure 27 Simulated daily O_3 concentration over Cape Town for the period 2001-2004. Extreme O_3 pollution events are identified as days on which O_3 levels exceeded the 99th percentile value (27 ppb) indicated by the horizontal dashed line.

Between 2001 and 2004, the simulated daily O_3 concentration over Cape Town exceeded the 99th percentile value on 13 days in different years and months (Figure 27). One extreme event occurred in January, five cases in March, six in April and one in September. However, only seven of these extreme pollution events (the one in January, three in March, two in April and the one September) are found to be associated with regional transport of air pollutants, while the other six extreme events show no evidence of regional implications, but rather are likely to be caused by atmospheric emissions over Cape Town.

Figure 28 shows the evolution of the regional distribution of O_3 concentration leading to extreme pollution levels over Cape Town, as a result of regional-scale transport of O_3 pollution. The figure shows a sequence of two days before the extreme O_3 pollution event occurs in Cape Town, the day with extreme O_3 concentration over Cape Town and a day after the extreme O_3 event. It is noteworthy that extreme O_3 levels over Cape Town are comparable to those over the industrial Highveld. In addition, there is an exceptional band of high O_3 concentration that forms along the southern coastline of South Africa, prior to the occurrence of an extreme O_3 event in Cape Town. The wind field suggests that this band results mainly from transported pollution from the Highveld region by northerly flows, that get trapped along the coastline, resulting in an accumulation of air pollutants. The coastal band acts as a reservoir of O_3 pollution that induces extreme levels over most of the south coast of South Africa and extends over Cape Town, especially when easterly flows from the Indian Ocean persist along the coastline. In April (Figure 28, E1-E2), the simulations suggest that O_3 pollution from the Highveld may also be directly transported to Cape Town by northeasterly winds with an anticyclonic pattern, comparable to berg winds over Cape Town (Jury et al., 1990). The O_3 transported to Cape Town might then contribute to increase local O_3 concentration. The termination of high O_3 incidences over Cape Town is characterized by a shift from winds of continental and coastal origin to winds of marine origin (Figure 28, Day +1). These winds are strong, such that they penetrate inland, bringing clean air from the ocean thus resulting in effective dilution of the air over Cape Town. The origin of these winds

is either the southwest or the southeast, suggesting that these flows correspond to frontal circulations and to "*The Cape Doctor*", respectively.

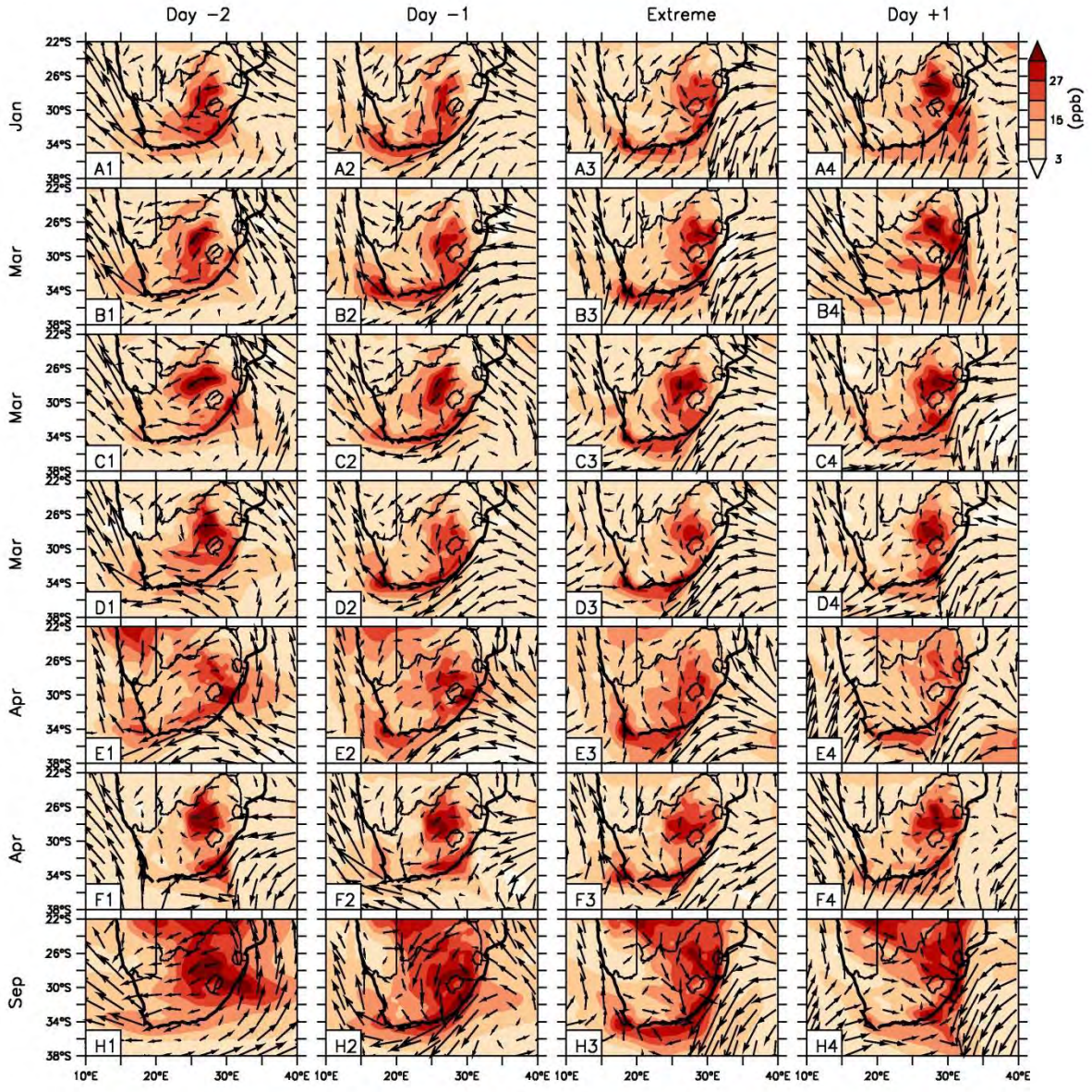

Figure 28 Cases of simulated extreme O_3 levels in Cape Town due to regional transport. The figure shows the spatial distribution of the O_3 simulated by RegCM and associated wind field for sequences of days linked to extreme O_3 levels over Cape Town. Each row represents a sequence of days, starting with two days before the extreme event (Day -2, Day -1), the day of the O_3 extreme event (Extreme) and the day after the extreme O_3 concentration over Cape Town (Day +1).

6.4 Paths of air parcels from the industrial Highveld to Cape Town

To investigate the transport of air parcels from the industrial Highveld to Cape Town, we consider — from the 1441 clusters of simulated lagrangian trajectories (see in Section 3.3) — clusters of trajectories that show a connection between the two locations. The identified trajectories are then classified into modes by similarity of pathways. Finally, each mode is associated with a frequency of occurrence with respect to the number of all identified cases.

With both WRF and RegCM results, the identified clusters of trajectories show that air pollutants with a relative long residence time in the troposphere, such as O_3, can reach Cape Town via four major pathways (Figure 29). Of all identified cases, the most frequent path (P1; 68.0% with WRF and 49.5% with RegCM) shows that air parcels from the industrial Highveld can reach Cape Town by the northeast route with an anticyclonic pattern (Figure 29a). This route suggests a pattern similar to that of the berg winds that have been associated with brown haze conditions in Cape Town (Jury et al., 1990). The second frequent path (P2; 18.0% with WRF and 30.1% with RegCM) by which O_3 can be advected from the industrial Highveld to Cape Town involves a deviation towards the southeast, followed by a shift towards tropical southern Africa, to reach Cape Town from the northwest (Figure 29b). This route is relatively long, such that the pollution from the industrial Highveld might affect tropical southern Africa more than downwind locations in South Africa. The third frequent path (P3; 13.4% with WRF and 19.0% with RegCM) shows that air parcels can reach Cape Town after being transported along the southern coastline (Figure 29c). Both the northeasterly

routes and the paths along the south coastline were shown to be associated with extreme O_3 levels (see in Section 6.2). Lastly, the least frequent path (P4; 0.6% with WRF and 1.4% with RegCM) shows that air parcels from the Highveld can be transported over the Indian Ocean, and then deviate to reach the region of Cape Town from the southwest (Figure 29d).

Furthermore, simulated trajectories with both models show that the regional transport of air parcels from the industrial Highveld to Cape Town can occur in any season, from summer (DJF) to spring (SON) (Tables 1 and 2). Nonetheless, both models agree that such a transport is less likely in summer when only 3.7% of the identified trajectories reach Cape Town. The simulated trajectories also show that air parcels from the industrial Highveld can reach Cape Town at a frequency of more than 40 days per year. While results with RegCM suggest that such a frequency varies between 46-67 days a year (Table 1), those with WRF show that such a transport may be less frequent, occurring on between 41-50 days per year (Table 2). In general, WRF simulates fewer cases than RegCM, especially in April, May and July. Nonetheless, because most of the identified trajectories occur on consecutive days, the transport of air parcels from the industrial Highveld to Cape Town is likely to contribute to a substantial increase of air pollutants over Cape Town, and thus to poor air quality in the city.

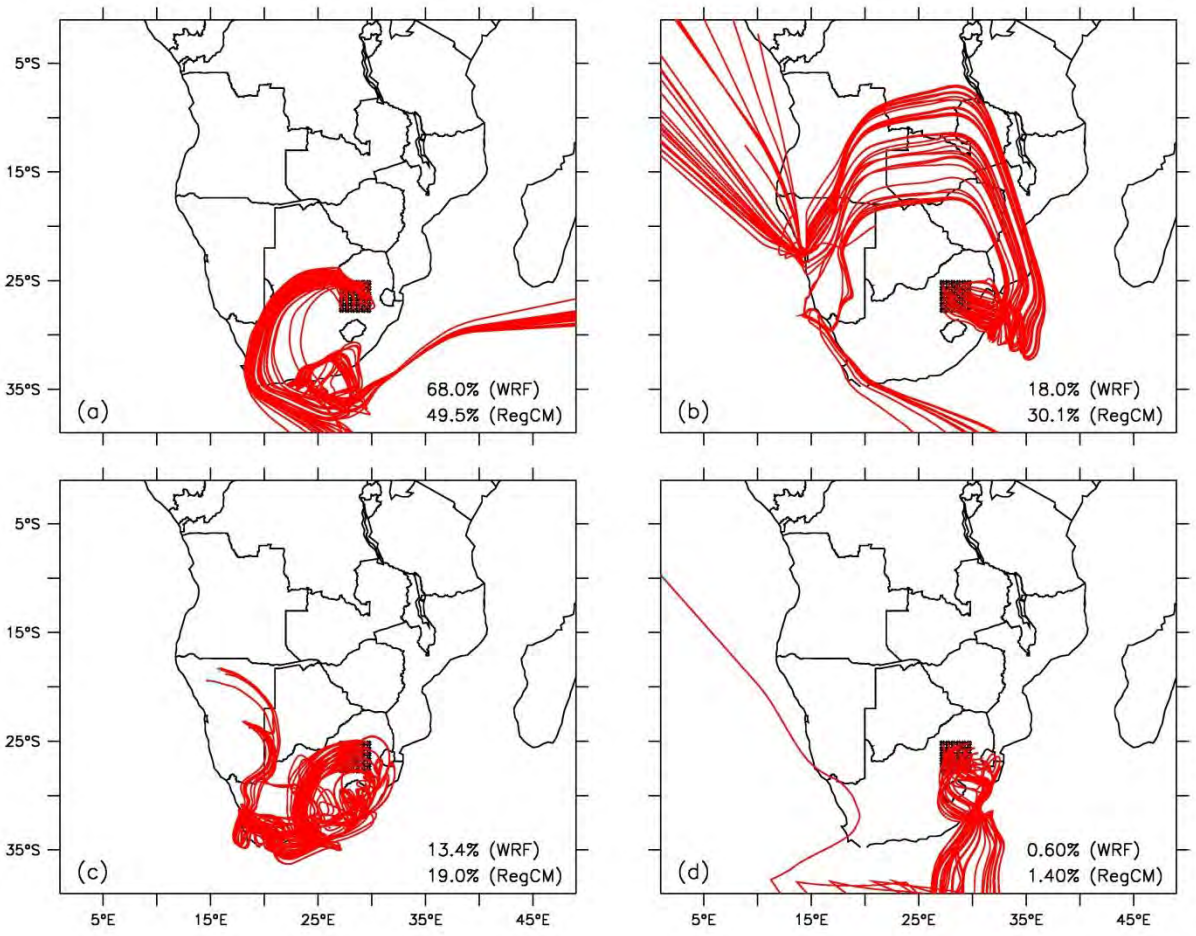

Figure 29 Advection paths of air parcels from the industrial Highveld to Cape Town.
(a) northeasterly path, (b) tropical deviation path, (c) southern coastline deviation path, and (d) oceanic deviation path. The frequency of occurrence of each transport mode (with respect to all identified cases) is given in the bottom left corner of each sub-figure.

Most importantly, both models suggest that more than 70% of the transport of air parcels from the industrial Highveld to Cape Town occurs between April and September, a period known to be characterized by poor dispersion conditions and the occurrence of brown haze over Cape Town (Piketh et al., 2004; Wicking-Baird et al., 1997; Jury et al., 1990). Under such atmospheric conditions, transported O_3 would then increase the local O_3 concentration and eventually lead to the occurrence of extreme pollution events in Cape Town.

Table 1 Occurrence of air transport from the Highveld to Cape Town with RegCM.
The table below shows the counts of days on which lagrangian trajectories simulated the advection of air parcels from the industrial Highveld to Cape Town. The paths P1, P2, P3 and P4 represent the northeasterly path, the tropical deviation path, the southern coastline path and the oceanic deviation path, respectively.

Year	Path	D	J	F	M	A	M	J	J	A	S	O	N	Total	
2001	P1	0	0	0	9	0	4	2	7	0	12	0	0	34	51
	P2	0	0	0	0	0	8	2	0	0	0	0	0	10	
	P3	0	0	0	2	1	0	0	0	0	4	0	0	7	
	P4	0	0	0	0	0	0	0	0	0	0	0	0	0	
2002	P1	0	0	0	0	0	3	1	6	2	4	0	0	16	52
	P2	0	0	0	3	3	7	0	11	2	3	0	0	29	
	P3	0	0	0	0	0	0	0	0	3	3	0	0	6	
	P4	0	0	0	0	0	1	0	0	0	0	0	0	1	
2003	P1	0	0	0	0	0	0	19	7	0	0	0	0	26	46
	P2	0	0	0	0	0	9	0	1	0	0	0	0	10	
	P3	0	0	0	0	0	3	5	0	0	0	0	0	8	
	P4	0	0	0	0	0	2	0	0	0	0	0	0	2	
2004	P1	0	0	0	1	2	13	2	6	0	1	6	0	31	67
	P2	0	0	2	0	5	4	5	0	0	0	0	0	16	
	P3	0	0	6	9	3	0	0	0	0	0	2	0	20	
	P4	0	0	0	0	0	0	0	0	0	0	0	0	0	
Total		0	0	8	24	14	54	36	38	7	27	8	0	216	

Table 2 Occurrence of air transport from the Highveld to Cape Town with WRF.
The table below shows the counts of days on which lagrangian trajectories simulated the advection of air parcels from the industrial Highveld to Cape Town. The paths P1, P2, P3 and P4 represent the northeasterly path, the tropical deviation path, the southern coastline path and the oceanic deviation path, respectively.

Year	Path	D	J	F	M	A	M	J	J	A	S	O	N	Total	
2001	P1	0	0	0	10	1	5	1	5	1	2	3	0	28	41
	P2	0	0	0	0	0	0	4	3	0	0	0	0	7	
	P3	0	0	0	2	1	0	0	0	0	2	0	1	6	
	P4	0	0	0	0	0	0	0	0	0	0	0	0	0	
2002	P1	0	0	1	3	0	7	6	2	2	1	0	0	22	45
	P2	0	0	2	0	3	5	1	1	1	2	0	0	15	
	P3	0	0	5	2	0	0	0	0	0	1	0	0	8	
	P4	0	0	0	0	0	0	0	0	0	0	0	0	0	
2003	P1	0	0	0	1	0	7	12	2	0	9	1	0	32	42
	P2	0	0	0	0	0	0	6	1	0	0	0	0	7	
	P3	0	0	0	0	0	2	0	0	0	0	0	0	2	
	P4	0	0	0	0	0	1	0	0	0	0	0	0	1	
2004	P1	0	0	0	7	2	7	3	5	4	5	6	0	39	50
	P2	0	0	0	0	0	3	0	0	0	0	0	0	3	
	P3	0	0	0	4	2	0	0	0	0	0	2	0	8	
	P4	0	0	0	0	0	0	0	0	0	0	0	0	0	
Total		0	0	8	29	9	37	33	19	8	22	12	1	178	

To recap on this analysis of lagrangian trajectories, both WRF and RegCM agree on the following results:

- The transport of air parcels from the industrial Highveld to Cape Town exists and can occur within 20 days. This transport may also occur in any season but it is less likely in summer.
- There exist four advection paths by which air pollutants from the industrial Highveld can be transported to Cape Town. The most frequent path is the direct northeasterly route, similar to berg winds over Cape Town. In addition, the paths associated with critical pollution over Cape Town are the direct northeasterly route and the path along the southern coastline of South Africa.
- The transport of pollutants from the industrial Highveld to Cape Town is relatively rare, but may occur at a frequency of more than 40 days per year. In most cases, the transport occurs on consecutive days, possibly leading to substantial increases of pollution levels over Cape Town.
- Finally, more than 70% of all identified cases occur between April and September, a period known to be characterized by poor air quality conditions (brown haze episodes) in Cape Town.

Chapter 7: Conclusion

7.1 Concluding summary

This dissertation focuses on O_3 pollution which has the potential to cause negative effects on vegetation, materials and human health. The aim of this study is to investigate the local variation and the regional-scale transport of O_3 pollution over Cape Town. This goal has been attained through the analyses of station data and simulated atmospheric pollution over southern Africa.

The results of the study can be summarized in the following points:

- In the Cape Town area, ground-level O_3 concentration increases during the daytime following sunlight driven production processes. On an episode day for example, ambient O_3 concentration in Cape Town may increase to reach 100 $\mu g/m^3$ for more than 8 consecutive hours in a day.
- The seasonal variation of ground-level O_3 concentration in the Cape Town area is strongly related to the prevailing wind conditions.
- The concentration of ground-level O_3 is higher at the remote background site (Cape Point) than at the urban site (Molteno) and the sub-urban site (Goodwood), mainly due to the presence of chemical sinks such as NO_x in the city.
- Both RegCM and WRF simulated the prevailing wind conditions over Cape Town well. The two models reproduced similar results, mainly because they were initialized with the same meteorological data.

- The set-up of the WRF model considered in this study accurately reproduces the variation of O_3, NO_x and wind variables over Cape Town. However, a problem was identified in the spatial distribution of photochemical pollutants (mainly O_3, CO and ethylene) over southern Africa. Hence the photochemical pollution simulated by WRF was not used to study the regional-scale transport of O_3 to Cape Town.
- On the other hand, the set-up of RegCM considered in this study provides credible simulations of the spatial and seasonal distribution of tropospheric O_3 concentration over South Africa. In fact, the simulations with RegCM reproduced well the regional spring O_3 maxima (Thompson et al., 1996a), highest levels of pollution over the industrial Highveld (Collett et al., 2000) and seasonal extreme pollution levels over the east coast of South Africa (Stein et al., 2003). Therefore, photochemical pollution simulated by RegCM was used to study the regional transport of O_3 pollution to Cape Town.
- The simulations by RegCM show that atmospheric emissions from the industrial Highveld can contribute to extreme O_3 concentration over Cape Town (especially in January, March, April and September) through the advection of O_3 pollution in the lowest layers of the atmosphere.

- Lagrangian trajectories simulated using wind outputs from both models (WRF and RegCM) show that there exist four major pathways by which air parcels from the industrial Highveld can be transported to Cape Town: a direct northeasterly path, a tropical deviation path, a deviation path along the southern coastline and a deviation path over the ocean.
- However, the study suggests that the paths linked to critical pollution over Cape Town are the direct northeasterly path and the path along the southern coastline.
- The climatology of the simulated trajectories suggests that the transport of air pollutants from the industrial Highveld to Cape Town occur rarely in a year (the frequency of occurrence is simulated to vary between 40-67 days per year). However, such a transport is simulated to occur mostly between April and September, which coincides with the season of brown haze episodes over Cape Town. Nevertheless, this study argues that the transported pollution to Cape Town contributes to increase the levels of air pollutants which are already substantial due to local emissions.

This study confirms the connection between atmospheric emissions from the industrial Highveld of South Africa and extreme pollution levels over Cape Town previously suggested by Abiodun et al. (2013) and Jenner and Abiodun (2013). Although the transport of air pollutants from the industrial Highveld to Cape Town seems to occur occasionally, the study recommends considering both the regional-scale emissions and transport in the monitoring of air quality in the city, especially between April and September.

7.2 Suggestions for further studies

There are various aspects of regional transport of air pollutants that still need to be investigated in order to better understand the sources of air pollution over Cape Town. Further studies should focus on the following points:

- A quantification of the contribution of atmospheric emissions from the industrial Highveld on pollutant levels over Cape Town would be necessary for scientific and policy-related assessment.
- The monitoring of the time along the different trajectories of air parcels from the industrial Highveld to Cape Town would be required to evaluate which pollutants can be transported between the two locations.
- Sampling or continuous measurements of pollutant concentrations along the most critical pathways (the direct northeasterly and southern coastline routes) would be useful in validating the identified transport routes.
- The use of remote sensing products may also contribute to strengthen the analysis of regional pollution and to evaluate of the identified transport patterns.
- The identification of other remote sources contributing to air pollution over Cape Town would also be of benefit to the local air quality monitoring service. These sources may be located over the subcontinent or as far as in South America (Brunke et al., 2004).
- If any study intends to use the WRF model to simulate the photochemical pollution over southern Africa, we recommend the use of other initial chemical emissions than EDGAR4.2. Alternative emission databases

include RETRO (Reanalysis of the tropospheric chemical composition over the past 40 years) (Schultz et al., 2007) and MOZART (Model for ozone and related chemical tracers) (Emmons et al., 2010).

7.3 Publication

Nzotungicimpaye, C.-M., Abiodun, B.J. and Steyn, D.G. (2014). Tropospheric ozone and its regional transport over Cape Town. *Atmospheric Environment*, 87: 228-238.

References

Abiodun, B.J., Ojumu, A.M., Jenner, S., and Ojumu, T.V. 2013. Transport of atmospheric NOx and HNO_3 over Cape Town. *Atmospheric Chemistry Physics*, 13: 11827-11862.

Andrea, M.O., Anderson, B.E., Blake, D.R., Bradshaw, J.D., Collins, J.E., Gregory, G.L., Sachse, G.W., and Shipham, M.C. 1994. Influence of plumes from biomass burning of atmospheric chemistry over the equatorial and tropical South Atlantic during CITE 3, *Journal of Geophysical Research*, 99: 12793-12808.

Atkinson, R. 2000. Atmospheric chemistry of VOCs and NO_x. *Atmospheric Environment*, 34: 2063-2141.

Avnery, S., Mauzerall, D.L., Liu, J., and Horrowitz, L.W. 2011. Global crop yield reductions due to surface ozone exposure: 1. Year 2000 crop production losses and economic damage. *Atmospheric Environment*, 45: 2284-2296.

Brankov, E., Henry, R.F., Civerolo, K.L., Hao, W., Rao, S.T., Misra, P.K., Bloxman, R., and Reid, N. 2003. Assessing the effect of transboundary ozone pollution between Ontario, Canada and New York, USA. *Environmental Pollution*, 123: 403-411.

Brunke, E.-G., Labuschagne, C., Parker, B., Scheel, H.E., and Whittlestone, S. 2004. Baseline air mass selection at Cape Point, South Africa: application of ^{222}Rn and other filter selection criteria to CO_2. *Atmospheric Environment*, 38: 5693–5702.

Borrego, C., Souto, J.A., Monteiro, A., Dios, M., Rodríguez, A., Ferreira, J., Saavedra, S., Casares, J.J., and Miranda, A.I. 2013. The role of transboundary air pollution over Galicia and North Portugal area. *Environmental Science and Pollution Research*, 20: 2924-2936.

Chiloane, K.E. 2005. *Volatile organic compounds analysis from Cape Town brown haze II study*. MSc thesis, University of the Witwatersrand.

City of Cape Town 2002. *State of the environment report for the City of Cape Town: Year 5 (2002)*. Cape Town.

——— 2005. *Air quality management plan for the City of Cape Town*. Cape Town.

——— 2012. 2011 Census – Cape Town Profile (December 2012). Compiled by Strategic Development Information and GIS and GIS Department, City of Cape Town, using 2011 Census data supplied by Statistics South Africa.

——— 2013. *Reports of air pollution episodes in Cape Town.* [Online]. Available at: http://web1.capetown.gov.za/web1/NewCityAirpol/reports.asp [Last access on: 1 October 2013].

Collins, W.J., Derwent, R.G., Johnson, C.E., and Stevenson, D.S. 2000. The impacts of human activities on the photochemical production and destruction of tropospheric ozone, *Quarterly Journal of the Royal Meteorological Society*, 126: 1925-1951.

Collett, K.S., Piketh, S.J., and Ross, K.E. 2010. An assessment of the atmospheric nitrogen budget on the South African Highveld. *South African Journal of Science*, 106 (5-6): 1-9.

Combrink, J., Diab, R.D., Sokolic F., and Brunke, E.-G. 1995. Relationship between surface, free tropospheric and total column ozone in two contrasting areas in South Africa. *Atmospheric Environment*, 29 (6): 685-691.

Cosijn, C., and Tyson, P.D. 1996. Stable discontinuities in the atmosphere over South Africa, *South African Journal of Science*, 92: 381-386.

Crétat, J., Pohl, B., Richard, Y., and Drobinski, P. 2011. Uncertainties in Simulating Regional Climate of Southern Africa: Sensitivity to Physical Parameterizations Using WRF. *Climate Dynamics*, 38 (3-4): 613–634.

Crutzen, P. 1974. Photochemical reactions initiated by and influencing O_3 in the unpolluted troposphere. *Tellus*, 26: 47-57.

Crutzen, P., and Zimmerman, P.H. 1991. The changing photochemistry of the atmosphere. *Tellus*, 43 (AB): 136-151.

Crutzen, P., Lawrence, M.G., and Pöschl, U. 1999. On the background photochemistry of tropospheric ozone. *Tellus*, 51 (A-B): 123-146.

D'Aberton, P.C. 1996. Lagrangian kinematic and isentropic trajectory models for aerosols and trace gas transport studies in southern Africa. *South African Journal of Science*, 92: 157-160.

Derwent, R.G., Stevenson, D.S., Collins, W.J., and Johnston, C.E. 2004. Intercontinental transport and the origins of the ozone observed at surface sites in Europe. *Atmospheric Environment*, 38: 1891-1901.

Derwent, R.G., Stevenson, D.S., Doherty, R.M., Collins, W.J., and Sanderson, M.G. 2008. How is surface ozone in Europe linked to Asian and North American NOx emissions? *Atmospheric Environment*, 42: 7412-7422.

Diab, R.D., Thompson, A.M., Zunckel, M., Coetzee, G.J.R., Combrink, J., Bodeker, G.E., Fishman, J., Sokolic, F., McNamara, D.P., and Archer, C.B. 1996. Vertical ozone distribution over southern Africa and adjacent oceans during SAFARI-92. *Journal of Geophysical Research*, 101 (D19): 23823-23833.

Dickerson, R.R., Kondragunta, S., Stenchikov, G., Civerolo, K.L., Doddridge, B.G., and Holben, B.N. 1997. The impacts of aerosols on solar ultraviolet radiation and photochemical smog. *Science*, 278: 827-830.

Dickinson, R.E., Henderson-Sellers, A., and Kennedy, P.J. 1993. *Biosphere-atmosphere transfer scheme (BATS) version 1e as coupled to the NCAR community climate model, Technical Report*. Boulder, Colorado.

Dudhia, J. 1989. Numerical study of convection observed during the winter monsoon experiment using a mesoscale two-dimensional model. *Journal of Atmospheric Chemistry*, 46: 3077–3107.

Duncan, B.N., West, J.J., Yoshida, Y., Fiore, A.M., and Ziemke, J.R. 2008. The influence of European pollution on ozone in the near East and northern Africa. *Atmospheric Chemistry Physics*, 8: 2267-2283.

Emmons, L.K., Walters, S., Hess, P.G., Lamarque, J.-F., Pfister, G.G., Fillmore, D., Granier, C., Guenther, A., Kinnison, D., Laepple, T., Orlando, J., Tie, X., Tyndall, G., Wiedinmyer, C., Baughcum, S.L., and Kloster, S. 2010. Description and evaluation of the Model for Ozone and Related Tracers, version 4 (MOZART-4). *Geoscientific Model Development*, 3: 43-67.

Ferris, B.G. 1978. Health effects of exposure to low level of regulated air pollutants: a critical review, *Journal of Air Pollution Control Association*, 28: 482-489.

Fiore, A.M., Jacob, D.J., Bey, I., Yantosca, R.M., Field, B.D., Fusco, A.C., and Wilkinson, J.G. 2002. Background ozone over the United States in summer: Origin, trend and contribution to pollution episodes. *Journal of Geophysical Research*, 107 (D15): DOI: 10.1029/2001JD000982.

Fishman, J., Minnis, P., and Reichle Jr., H.G. 1986. The use of satellite data to study tropospheric ozone in the tropics. *Journal of Geophysical Research*, 91: 14541-14645.

Fishman, J., and Larsen, J.C. 1987. Distribution of total ozone and stratospheric ozone in the tropics: Implications for the distribution of tropospheric ozone. *Journal of Geophysical Research*, 92: 6627-6634.

Fishman, J., Watson, C.E., Larsen, J.C., and Logan, J.A. 1990. The distribution of tropospheric ozone determined from satellite data. *Journal of Geophysical Research*, 95: 3599-3617.

Fishman, J., Fakhruzzaman, K., Cros, B., and Nganga, D. 1991. Identification of widespread pollution in the Southern Hemisphere deduced from satellite analyses. *Science*, 252: 1693-1696.

Freiman, M.T., and Piketh, S.J. 2002. Air transport into and out of the Industrial Highveld Region of South Africa. *Journal of Applied Meteorology*, 42: 994-1002.

Freitas, S.R., Longo, K.M., Alonso, M.F., Pirre, M., Marecal, V., Grell, G., Stockler, R., Mello, R.F., and Gácita, M.S. 2011. PREP-CHEM-SRC — 1.0: a preprocessor of trace gas and aerosol emission fields for regional and global atmospheric chemistry models. *Geoscientific Model Development*, 4: 419-433.

Fritsch, J.M., and Chappell, C.F. 1980. Numerical prediction of convectively driven mesoscale pressure systems, Part 1: Convective parameterization. *Journal of Atmospheric Science*, 37: 1722-1733.

Garstang, M., Tyson, P.D., Swap, R.J., Kållberg, E.P., and Lindesay, J.A. 1996. Horizontal and vertical transport of air over southern Africa, *Journal of Geophysical Research*, 101 (D19): 23721-23736.

Grell, G.A., and Dévényi, D. 2002. A generalized approach to parameterizing convection combining ensemble and data assimilation techniques. *Geophysical Research Letters*, 29: No 14, 1693.

Grell, G.A., Peckham, S.E., Schmitz, R., McKeen, S.A., Frost, G., Skamarock, W.C., and Eder, B. 2005. Fully coupled online chemistry within the WRF model. *Atmospheric Environment*, 39: 6957-6975.

Giorgi, F., and Anyah, R.O. 2012. The road towards RegCM4. *Climate Research*, 52: 3-6.

Holtslag, A.A.M., and Boville, B.A. 1993. Local versus nonlocal boundary-layer diffusion in a global climate model. *Journal of Climate*, 6: 1825-1842.

Hong, S., Noh, Y., and Dudhia, J. 2006. A new vertical diffusion package with an explicit treatment of entrainment processes. *Monthly Weather Review*, 134: 2318-2341.

Jenner, S., and Abiodun, B.J. 2013. The transport of atmospheric sulfur over Cape Town. *Atmospheric Environment*, 79: 248-260.

Jury, M., and Spencer-Smith, G. 1988. Doppler sounder observations of trade winds and sea breezes along the African west coast near 34°S, 19°E. *Boundary Layer Meteorology*, 34: 373-405.

Jury, M., Tegen, A., Ngeleza, E., and Du Toit, M. 1990. Winter air pollution episodes over Cape Town. *Boundary Layer Meteorology*, 53: 1-20.

Kalognomou, E.-A., 2009. *Air quality and climate change over the Greater Cape Town area*. MSc thesis, University of Cape Town.

Kiehl, J.T., Hack, J.J., Bonan, G.B., Boville, B.A., Briegleb, B.P., Williamson, D.L., and Rasch, P.J. 1996. *Description of the NCAR community climate model (CCM3), Technical Report.* Boulder, Colorado.

Keen, C.S. 1979. *Meteorological aspects of pollution transport over the south-western Cape, Technical Report*. Department of Geography, University of Cape Town.

Lee, D.S., Holland, M.R., and Falla, N. 1996. The potential impact of ozone on materials in the U.K. *Atmospheric Environment*, 35: 1053-1065.

Li, Q., Jacob, D.J., Bey, I., Palmer, P.I., Duncan, B.N., Field, B.D., Martin, R.V., Fiore, A.M., Yantosca, R.M., Parrish, D.D., Simmonds, P.G., and Oltmans, S.J. 2002. Transantlatic transport of pollution and its effects on surface ozone in Europe and North America. *Journal of Geophysical Research*, 107 (D13): 4166, 10.1029/2001JD001422.

Lippman, M. 1989. Health effects of ozone: A critical review. *Journal of the Air and Waste Management Association*, 39: 672-695.

Liu, S.C., Kley, D., McFarland, M., Mahlman, J.D., and Levy II, H. 1980. On the origin of tropospheric ozone. *Journal of Geophysical Research*, 85: 7546-7552.

Liu, J., and Mauzerall, D.L. 2005. Estimating the average time for inter-continental transport of air pollutants. *Geophysical Research Letters*, 32: L11814, DOI: 10.1029/2005GL022619, 2005.

Madronich, S. 1987. Photodissociation in the Atmosphere: 1. Actinic Flux and the Effects of Ground Reflections and Clouds. *Journal of Geophysical Research*, 92: 9740–9752.

Madronich, S., and Flocke, S. 1999. "The role of solar radiation in atmospheric chemistry". In *Handbook of Environmental Chemistry*. Ed. P. Boule, 1-26. New York: Springer-Verlag.

Massey, S.W. 1999. The effects of ozone and NOx on the deterioration of calcareous stone. *Science of the Total Environment*, 227 (2–3): 109–121.

Mlawer, E.J., Taubman, S.J., Brown, P.D., Iacono, J., and Clough, S.A. 1997. Radiative transfer for inhomogeneous atmospheres: RRTM, a validated correlated-k model for the longwave. *Journal of Geophysical Research*, 102 (16): 663–682.

Monin, A.S., and Obukhov, A.M. 1954. Basic laws of turbulent mixing in the atmosphere near the ground. *Trudy Institute Geologicheskikh* 24 (151): 163-187.

Monteiro, A., Strunk, A., Carvalho, A., Tchepel, O., Miranda, A.I., Borrego, C., Saavedra, S., Rodríguez, A., Souto, J., Casares, J., Friese, E., and Elbern, H. 2012. Investigating a high ozone episode in a rural mountain site. *Environmental Pollution*, 162: 176-189.

Munnik, V., Hochmann, G., Hlabane, M., and Law, S. 2010. *The social and environmental consequences of coal mining in South Africa: A case study.* Environmental Monitoring Group, Cape Town, pages 24.

Oltmans, S.J., 1981. Surface ozone measurements in clean air. *Journal of Geophysical Research*, 86: 1174-1180.

Oltmans, S.J., and Levy II, H. 1994. Surface ozone measurements from a global network. *Atmospheric Environment*, 28: 9-24.

Pal, J.S., Giorgi, F., Bi, X., Elguindi, N., Solmon, F., Gao, X., Rauscher, S.A., Francisco, R., Zakey, A., Winter, J., Ashfaq, M., Syed, F.S., Bell, J.L., Diffenbaugh, N.S., Karmacharya, J., Konaré, A., Martinez, D., da Rocha, R.P., Sloan, L.S., and Steiner, A.L. 2007. Regional Climate Modeling for the Developing World: The ICTP RegCM3 and RegCNET. *Bulletin of the American Meteorological Society*, 88 (9): 1395-1409.

Paolleti, E. 2009. Ozone and urban forests in Italy. *Environmental Pollution*, 157: 1506-1512.

Piketh, S.J., Swap, R.J., Maenhaut, W., Annegram, H.J., and Formenti, P. 2002. Chemical evidence of long-range atmospheric transport over southern Africa. *Journal of Geophysical Research*, 107 (D24): 4817, DOI: 10.1029/2002JD002056.

Piketh S.J., Otter, L., Burger, R.P., Walton, N., Van Nierop, M.A., Bigala, T., Chiloane K.E., and Gwaze, P. 2004. *Brown haze II Report, Cape Town.* Cape Town, pages 81.

Preston-Whyte, R.A., Diab, R.D., and Tyson, P.D. 1977. Towards an inversion climatology of southern Africa, II, Non-surface inversions in the lower atmosphere. *South African Geographical Journal*, 59: 47-59.

Preston-Whyte, R.A. and Tyson, P.D. 1988. *The atmosphere and weather of southern Africa*. Cape Town: Oxford University Press.

Salby, M.L. 1996. *Fundamentals of atmospheric physics*. London, UK: Academic Press.

Saavedra, S., Rodriguez, A., Taboada, J.J., Souto, J.A., and Casares, J.J. 2012. Synoptic patterns and air mass transport during ozone episodes in northwestern Iberia. *Science of the Total Environment*, 412: 97-110.

Scheel, H.-E., Sladkovic, R., Brunke, E.-G., Selier, W. 1990. Trace gas measurements at the monitoring station, Cape Point, South Africa, between 1978-1988, *Journal of Atmospheric Chemistry*, 11: 197-210.

Schultz, M.G., Backman, L., Balkanski, Y., Bjoerndalsaeter, S., Brand, R., Burrows, J.P., Dalsoeren, S., De Vasconcelos, M., Grodtmann, B., Hauglustaine, D.A., Heil, A., Hoelzemann, J.J., Isaksen, I.S.A., Kaurola, J., Knorr, W., Ladstaetter-Weißenmayer, A., Mota, B., Oom, D., Pacyna, J., Panasiuk, D., Pereira, J.M.C., Pulles, T., Pyle, J., Rast, S., Richter, A., Savage, N., Schnadt, C., Schulz, M., Spessa, A., Staehelin, J., Sundet, J.K., Szopa, S., Thonicke, K., Van het Bolscher, M., Van Noije, T., Van Velthoven, P., Vik, A.F., and Wittrock, F. 2007. *Reanalysis of the Tropospheric chemical composition over the past 40 years (RETRO): A long-term global modeling study of tropospheric chemistry, Final Report*. Hamburg, Germany.

Scorgie, Y. and Raylene, W. 2004. *Updated Air Quality Situation Assessment for the City of Cape Town, Technical Report*. Airshed Planning Professionals (Pty) Ltd. Johannesburg, Gauteng.

Shalaby, A., Zakey, A., Tawfik, A.B., Solmon, F., Giorgi, F., Stordal, F., Sillman, S. Zaveri, R.A., and Steiner, A.L. 2012. Implementation and evaluation of online gas-phase chemistry within a regional climate model (RegCM-CHEM4). *Geoscience Model Development*, 5: 741-760.

Sillman, S. 1999. The relation between ozone, NOx and hydrocarbons in urban and polluted rural environments. *Atmospheric Environment*, 33: 1821-1845.

Sillman, S. 2003. Tropospheric ozone and photochemical smog. In *Treatise on Geochemistry, Vol. 9*. Ed. H.D. Holland and K.K. Turekian. pp. 612. ISBN 0-08-043751-6. Elsevier, pp. 407-431.

Skamarock, W.C., Klemp, J.B., Dudhia, J., Gill, D.O., Barker, D.M., Wang, W., and Powers, J.G. 2005. *A Description of the Advanced Research WRF Version 2. NCAR Technical Note.* Boulder, Colorado.

Sowden, M., Cairncross, E., Wilson, G., Zunckel, M., Kirillova, E., Reddy, V., and Hietkamp, S. 2008. Developing a spatially and temporally resolved emission inventory for photochemical modeling in the City of Cape Town and assessing its uncertainty. *Atmospheric Environment*, 42: 7155-7164.

Stein D.C., Swap, R.J., Greco, S., Piketh, S.J., Macko, S.A., Doddridge, B.C., Elias, T., and Bruintjes R.T. 2003. Haze layer characterization and associated meteorological controls along the eastern coastal region of southern Africa. *Journal of Geophysical Research* 108 (D13), 8506, doi:10.1029/2002JD003237.

Stevenson, D.S., Dentener, F.J., Schultz, M.G., Ellingsen, K., Van Noije, T.P.C., Wild, O., Zeng, G., Amann, M., Atherton, C.S., Bell, N., Bergmann, D.J., Bey, I., Butler, T., Cofala, J., Collins, W.J., Derwent, R.G., Doherty, R.M., Drevet, J., Eskes, H.J., Fiore, A.M., Gauss, M., Hauglustaine, D.A., Horowitz, L.W., Isaksen, I.S.A., Krol, M.C., Lamarque, J.-F., Lawrence,

M.G., Montanaro, V., Müller, J.-F., Pitari, G., Prather, M.J., Pyle, J.A., Rast, S., Rodriguez, J.M., Sanderson, M.G., Savage, N.H., Shindell, D.T., Strahan, S.E., Sudo, K., and Szopa, S. 2006. Multimodel ensemble simulations of present-day and near-future tropospheric ozone. *Journal of Geophysical Research*, 111: D08301, DOI: 10.1029/2005JD006338.

Stohl, A., Eckhardt, S., Forster, C., James, P., and Spichtinger, N. 2002. On the pathways and timescales of intercontinental air pollution transport. *Journal of Geophysical Research*, 107 (D23): 4684, DOI: 10.1029/2001JD001396.

Sturman, A.P., Tyson, P.D., and D'Aberton, P.C. 1997. A preliminary study of the transport of air from Africa and Australia to New Zealand. *Journal of the Royal Society of New Zealand*, 27: 485-498.

Swap, R.J., Garstang, M., Tyson, P.D., Maenhaut, W., Artaxo, P., Kållberg, P., and Talbot, P. 1996. The long-range transport of southern African aerosols to the tropical South Atlantic. *Journal of Geophysical Research*, 101 (D19): 23777-23791.

Swap, R.J., Szuba, T.A., Garstang, M., Annegram, H.J., Marufu, L., and Piketh, S.J. 2003. Spatial and temporal assessment of sources contributing to the annual austral spring mid-tropospheric ozone maxima over the tropical South Atlantic. *Global Change Biology*, 9: 336-345.

Sylla, M.B., Coppola, E., Mariotti, L., Giorgi, F., Ruti, P.M., Dell'Aquila, A., and Bi, X. 2009. Multiyear simulation of the African climate using a regional climate model (RegCM3) with the high resolution ERA-interim reanalysis. *Climate Dynamics*, 35 (1): 231–247.

Tessema, M.A. 2011. *Particulate matter (PM10) pollution in Khayelitsha, Cape Town*. Essay, African Institute for Mathematical Sciences, South Africa.

The Royal Society 2008. *Ground-level ozone in the 21st century: future trends, impacts and policy implications, Technical Report.* London, UK.

Thompson, A.M., Pickering, K.E., McNamara, D.P., Schoeberl, M.R., Hudson, R.D., Kim, J.H., Browell, E.V., Kirchhoff, V.W.J.H., and Nganga, D. 1996a. Where did tropospheric ozone over southern Africa and the tropical Atlantic come from in October 1992? Insights from TOMS, GTE TRACE A, and SAFARI 1992. *Journal of Geophysical Research*, 101 (D19): 24251-24278.

Thompson A.M., Diab, R.D., Bodeker, G.E., Zunckel, M., Coetzee, G.J.R., Archer, C.B., McNamara, D.P., Pickering, K.E., Combrink, J., Fishman J., and Nganga, D. 1996b. Ozone over southern Africa during SAFARI-92/TRACE A. *Journal of Geophysical Research*, 101 (D19): 23793-23807.

Tyson, P.D., Garstang, M., Swap, R.J., Kållberg, P., and Edwards, M. 1996. An air transport climatology for subtropical southern Africa. *International Journal of Climatology*, 16: 265-291.

Tyson, P.D, Garstang, M., Thompson, A.M., Diab, R.D., and Browvell, E.V. 1997. Atmospheric transport and photochemistry of ozone over central southern Africa during the Southern Africa Fire-Atmosphere Research Initiative. *Journal of Geophysical Research*, 102 (D9): 10623-10635.

Tyson, P.D., and Gatebe, C.K. 2001. The atmosphere, aerosols, trace gases and biogeochemical change in Southern Africa: A regional integration. *South African Journal of Science*, 97: 106-118.

Unger, N., Menon, S., Koch, D.M., and Shindell, D.T. 2009. Impacts of aerosol-cloud interactions on past and future changes in tropospheric composition. *Atmospheric Chemistry Physics*, 9: 4115-4130.

Van Tienhoven, A.M., Zunckel, M., Emberson, L., Koosialee, A., and Otter, L. 2006. Preliminary assessment of risk of ozone impacts to maize (Zea mays) in Southern Africa. *Environmental Pollution*, 140: 220-230.

Walton, N.M. 2005. *Characterisation of Cape Town Brown Haze.* MSc thesis, University of the Witwatersrand.

Wenig, M., Spichtinger, N., Stohl, A., Held, G., Beirle, S., Wagner, T., Jähne, B., and Platt, U. 2003. Intercontinental transport of nitrogen oxide pollution plumes. *Atmospheric Chemistry Physics*, 3: 387-393.

Wesley, M.L. 1989. Parameterization of surface resistance to gaseous dry deposition in regional-scale numerical models. *Atmospheric Environment,* 23: 1293-1304.

Wichmann, J., and Voyi, K. 2012. Ambient air pollution exposure and respiratory, cardiovascular and cerebrovascular mortality in Cape Town, South Africa: 2001-2006. *International Journal of Environmental Research and Public Health*, 9: 3978–4016.

Wicking-Baird, M.C., De Villiers, M.G., and Dutkiewicz, R.K. 1997. *Cape Town Brown Haze Study, Report No. Gen 182*. Energy Research Institute, Cape Town, pages 78.

WHO (World Health Organization) 2006. *WHO air quality guidelines for particulate matter, ozone, nitrogen dioxide and sulfur dioxide: Summary of risk assessment*. Geneva, Switzerland.

Yoshitomi, M., Wild, O., and Akimoto, H. 2011. Contributions of regional and intercontinental transport to surface ozone in the Tokyo area. *Atmospheric Chemistry Physics*, 11: 7583-7599.

Zaveri, R.A., and Peters, L.K. 1999. A new lumped structure photochemical mechanism for long-scale applications. *Journal of Geophysical Research*, 30: 387-415.

Zunckel, M., Robertson, L., Tyson, P.D., and Rodhe, H. 2000. Modelled transport and deposition of sulphur over southern Africa. *Atmospheric Environment*, 34: 2797-2808.

Zunckel, M., Venjonoka, K., Pienaar, J.J., Brunke, E.-G., Pretorius, O., Koosialee, A., Raghunandan, A., and Van Tienhoven, A.M. 2004. Surface ozone over southern Africa: synthesis of monitoring results during the Cross border Air Pollution Impacts Assessment project. *Atmospheric Environment*, 38: 6139-6147.

Zunckel, M., Koosialee, A., Yarwood, G., Maure, G., Venjonoka, K., Van Tienhoven, A.M., and Otter, L. 2006. Modelled surface ozone over southern Africa during the Cross border Air Pollution Impacts Assessment project. *Environmental Modelling and Software*, 21: 911-924.